

Physical interactions among flavonoid enzymes in snapdragon and torenia reveal the diversity in the flavonoid metabolon organization of different plant species

Naoto Fujino^{1,†}, Natsuki Tenma^{1,†}, Toshiyuki Waki¹, Keisuke Ito¹, Yuki Komatsuzaki¹, Keigo Sugiyama¹, Tatsuya Yamazaki¹, Saori Yoshida¹, Masayoshi Hatayama¹, Satoshi Yamashita^{1,‡}, Yoshikazu Tanaka², Reiko Motohashi³, Konstantin Denessiouk⁴, Seiji Takahashi¹ and Toru Nakayama^{1,*}

¹Graduate School of Engineering, Tohoku University, Aza Aoba, Aramaki, Aoba 6-6-11, Sendai, Miyagi 980-8579, Japan,

²Suntory World Research Center, Suntory Holdings Ltd., Soraku-gun, Kyoto 619-0284, Japan,

³Department of Biological and Environmental Science, Faculty of Agriculture, Shizuoka University, Shizuoka 422-8529, Japan, and

⁴Department of Biosciences, Åbo Akademi University, Turku 20520, Finland

Received 15 December 2016; revised 4 January 2018; accepted 31 January 2018; published online 8 February 2018.

*For correspondence (e-mail nakayama@seika.che.tohoku.ac.jp).

†N.F. and N.T. were equal contributors to this paper.

‡Present address: Graduate School of Natural Science and Technology, Kanazawa University, Kanazawa 920-1192, Japan.

SUMMARY

Flavonoid metabolons (weakly-bound multi-enzyme complexes of flavonoid enzymes) are believed to occur in diverse plant species. However, how flavonoid enzymes are organized to form a metabolon is unknown for most plant species. We analyzed the physical interaction partnerships of the flavonoid enzymes from two lamiales plants (snapdragon and torenia) that produce flavones and anthocyanins. In snapdragon, protein–protein interaction assays using yeast and plant systems revealed the following binary interactions: flavone synthase II (FNSII)/chalcone synthase (CHS); FNSII/chalcone isomerase (CHI); FNSII/dihydroflavonol 4-reductase (DFR); CHS/CHI; CHI/DFR; and flavonoid 3'-hydroxylase/CHI. These results along with the sub-cellular localizations and membrane associations of snapdragon flavonoid enzymes suggested that FNSII serves as a component of the flavonoid metabolon tethered to the endoplasmic reticulum (ER). The observed interaction partnerships and temporal gene expression patterns of flavonoid enzymes in red snapdragon petal cells suggested the flower stage-dependent formation of the flavonoid metabolon, which accounted for the sequential flavone and anthocyanin accumulation patterns therein. We also identified interactions between FNSII and other flavonoid enzymes in torenia, in which the co-suppression of FNSII expression was previously reported to diminish petal anthocyanin contents. The observed physical interactions among flavonoid enzymes of these plant species provided further evidence supporting the long-suspected organization of flavonoid metabolons as enzyme complexes tethered to the ER via cytochrome P450, and illustrated how flavonoid metabolons mediate flower coloration. Moreover, the observed interaction partnerships were distinct from those previously identified in other plant species (*Arabidopsis thaliana* and soybean), suggesting that the organization of flavonoid metabolons may differ among plant species.

Keywords: metabolon, protein–protein interaction, cytochrome P450, flavonoid, anthocyanin, aurone, flavone synthase II, *Antirrhinum majus* L., *Torenia hybrida*.

INTRODUCTION

The cell cytoplasm is crowded with soluble macromolecules, structural elements (e.g. the cytoskeleton) and membranes, as well as small solute molecules (Fulton, 1982). This cytoplasmic ‘molecular crowding’ potentially provides intracellular diffusive barriers against macromolecules and small solutes (Verkman, 2002). One of the

cellular strategies to overcome such a mechanistic disadvantage in metabolism is to form a ‘metabolon’ (Ovadi and Srere, 2000; Ovadi and Saks, 2004; Jorgensen *et al.*, 2005; Srere, 2000). The metabolon is a fragile, highly organized super-molecular complex of metabolic enzymes (Ovadi and Srere, 2000; Srere, 2000). Metabolons have been proposed

to form on cellular structural elements, such as the cytoskeleton and cellular membrane systems, including the endoplasmic reticulum (ER; Ralston and Yu, 2006). Intracellular metabolic flux is facilitated by the metabolon because it permits the 'micro-compartmentalization' of metabolism in the cell (Ovadi and Saks, 2004; Sweetlove and Fernie, 2013), where a group of enzymes and metabolites in the metabolic pathway is concentrated in a small local area of the cell. It may also permit 'metabolite channeling' (Ovadi, 1991; Ovadi and Srere, 2000), which refers to the transfer of the reaction product of one enzyme to the next enzyme without equilibrating in the bulk solution. The dynamic formation and dissociation of metabolons may contribute to the mechanism responsible for regulating metabolism (Bassard *et al.*, 2017; Crosby *et al.*, 2011; Graham *et al.*, 2007; Laursen *et al.*, 2015, 2016; Møller, 2010).

Flavonoids are an important group of specialized plant metabolites, which are critical for plant survival and reproduction, and are relevant for human nutrition. The 10 major flavonoid classes (i.e. chalcones, aurones, flavanones, flavones, isoflavones, dihydroflavonols, flavonols, leucoanthocyanidins, anthocyanins and proanthocyanidins; see Figure 1 for some of their structures) include more than 8000 different structures in plants (Andersen and Markham, 2006). This structural diversity is believed to be the consequence of plant species adapting to specific ecological niches (Mouradov and Spangenberg, 2014). Thus, although flavonoid biosynthetic pathways are highly conserved among seed plants, each plant lineage developed structurally distinct flavonoids in a lineage-specific manner. These flavonoids were the result of the novel functions of biosynthetic enzymes that enhanced plant fitness under specific environmental conditions. The diversity in flavonoid structures may arise from the combined effects of flavonoid biosynthesis enzymes (flavonoid enzymes) with different catalytic functions and specificities (Noguchi *et al.*, 2009; Weng, 2014).

The formation of metabolons related to plant flavonoid biosynthesis (flavonoid metabolons) was first proposed in 1974 (Stafford, 1974), and was subsequently supported by several lines of experimental evidence (Hrazdina and Wagner, 1985; Hrazdina *et al.*, 1987; Winkel, 2004). Since then, flavonoid metabolons have been assumed to occur in diverse plant species. However, flavonoid metabolons have yet to be comprehensively characterized, and it remains unclear which enzymes and proteins are bound to each other and how they are organized. Thus far, only a few plant species have been studied regarding the existence of flavonoid metabolons. These studies have involved analyses of protein–protein interactions among flavonoid enzymes. In *Arabidopsis thaliana*, which constitutively produces flavonols and proanthocyanidins, physical interaction partnerships among cytoplasmic flavonoid enzymes [chalcone synthase (CHS), chalcone isomerase (CHI),

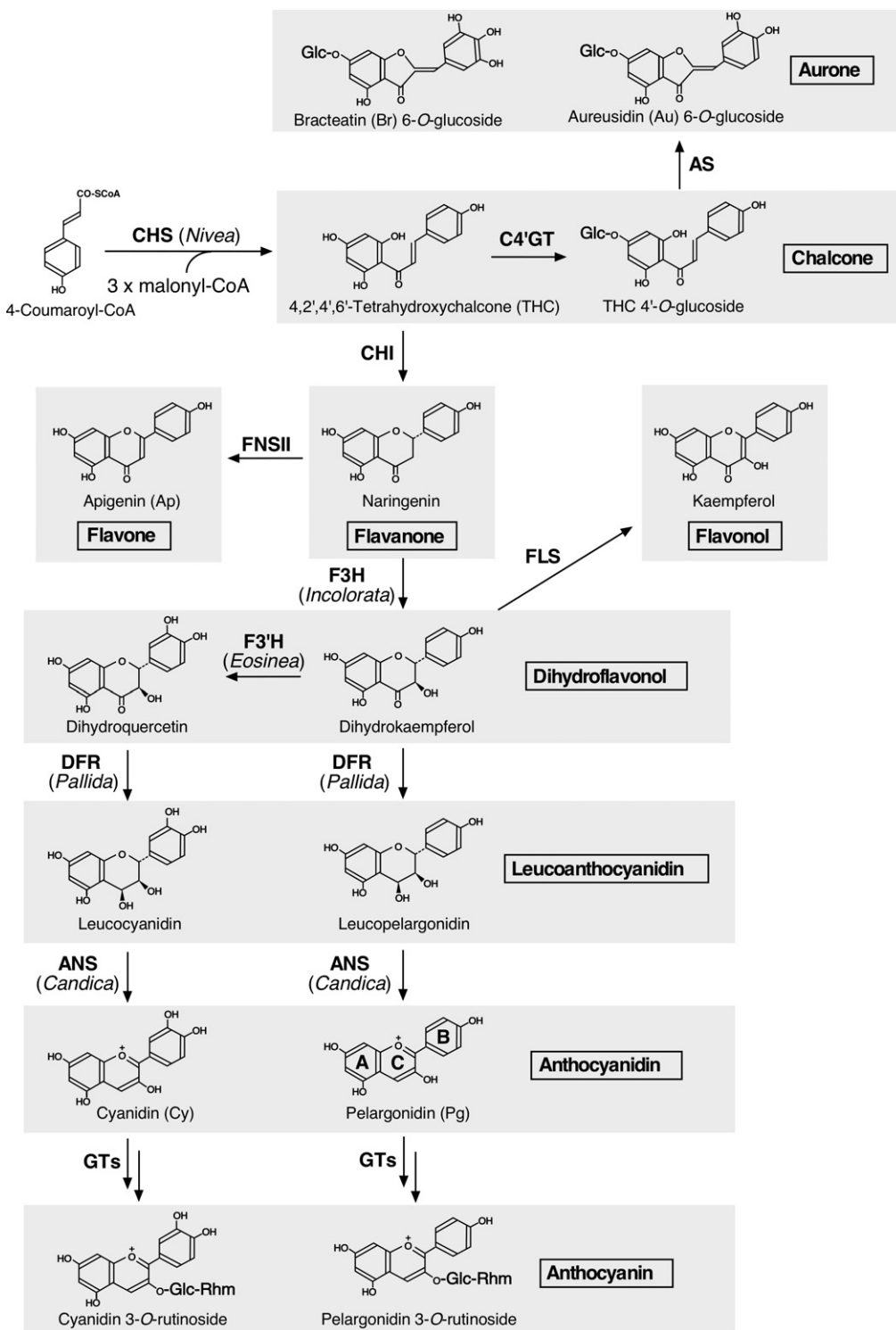
flavanone 3-hydroxylase (F3H), dihydroflavonol 4-reductase (DFR), and flavonol synthase (FLS)] have been revealed using molecular biological, immunological and physico-chemical methods (Winkel-Shirley, 1999; Crosby *et al.*, 2011). Two recent studies on *Glycine max*, which characteristically accumulates isoflavones, confirmed that P450 enzymes (i.e. 2-hydroxyisoflavanone synthase and cinnamate 4-hydroxylase) are important metabolon components for isoflavone biosynthesis (Dastmalchi *et al.*, 2016; Waki *et al.*, 2016). These findings provide further evidence that P450 proteins serve as metabolon components related to plant specialized metabolism. Specifically, P450s anchor soluble enzymes to form an enzyme complex tethered to the ER, as previously proposed based on metabolon studies involving lignin and cyanogenic glucoside pathways (Bassard *et al.*, 2012, 2017; Møller, 2010; Laursen *et al.*, 2016). However, despite the observed conservation and diversity of flavonoid pathways in plants, direct protein interactions among flavonoid enzymes have been demonstrated for only *A. thaliana* and *G. max*. The common (if any) and unique features of flavonoid metabolons among diverse plant species and lineages must still be elucidated.

In this study, we comprehensively analyzed protein–protein interactions between flavonoid enzymes in snapdragon (*Antirrhinum majus* L.) and in a related plant species (*Torenia hybrida*) to examine the potential formation of flavonoid metabolons in petal cells. These plants are flowering ornamentals in which large colorful petals are the most eye-catching trait (Hudson *et al.*, 2008; Ueyama *et al.*, 2002; Sasaki and Nakayama, 2015; Schwarz-Sommer *et al.*, 2003). The flower petal colors in these two species are provided by flavonoids, including anthocyanins (red to reddish purple in snapdragon and torenia), aurones (yellow in snapdragon; Nakayama *et al.*, 2000, 2001) and flavones [co-pigments in snapdragon (Asen *et al.*, 1972) and torenia; Figure 1]. These represent different flavonoid classes from those mainly found in *A. thaliana* and *G. max*. We also analyzed the membrane association and temporal gene expression of snapdragon flavonoid enzymes, and quantified floral pigments. Our results strongly suggest there are metabolons related to the production of flavones and anthocyanins in these plant species. Our data represent important information regarding the lineage-specific aspects of flavonoid metabolon structures and functions in plants.

RESULTS

Identification of binary interactions between snapdragon flavonoid enzymes using yeast assay systems

Because P450 proteins are believed to be important components of metabolons involved in specialized plant metabolic pathways, we first screened protein–protein interactions between flavonoid enzymes and P450s

**Figure 1.** Flavonoid biosynthesis in snapdragon petals.

Flavonoid names are provided under chemical structures. Flavonoid classes are presented with shadowed rectangles, with class names in boxes. Abbreviated enzyme names are as follows: CHS, chalcone synthase; C4'GT, chalcone 4'-glucosyltransferase; AS, aureusidin synthase; CHI, chalcone isomerase; FNSII, flavone synthase II; F3H, flavanone 3-hydroxylase; DFR, dihydroflavonol 4-reductase; ANS, anthocyanidin synthase; GTs, glycosyltransferases; FLS, flavonol synthase; F3'H, flavonoid 3'-hydroxylase. The CHS, DFR, ANS and F3H gene locus names are provided in parentheses. Note that F3'H can also use naringenin as a substrate (not shown in this figure). Flavones identified in the Cy-accumulating petals analyzed in this study were luteolin and chrysoeriol (structures not shown). In snapdragon petals, flavones and flavonols occur as 7-O-glucuronides and 3-O-glucosides, respectively, which are produced by various glycosyltransferases (Noguchi *et al.*, 2009). Glc, glucosyl; Rhm, rhamnosyl.

associated with the snapdragon flavonoid pathway. In this pathway (Figure 1), flavones synthase II [FNSII; AmFNSII (CYP93B1) (Akashi *et al.*, 1999)] and F3'H [AmF3'H (CYP75B) or Eosinea (Stickland and Harrison, 1974; Forkmann and Stotz, 1981)] are P450 proteins that contain an N-terminal sequence anchoring them to the ER membrane (Tanaka and Brugliera, 2013). Thus, a split-ubiquitin (SU) system (Iyer *et al.*, 2005) was used to screen for interactions between these P450 proteins and other soluble flavonoid enzymes in snapdragon [i.e. CHS (AmCHS1 or Nivea) (Hatayama *et al.*, 2006); CHI (AmCHI1) (Fujino *et al.*, 2014); F3H (AmF3H or Incolorata); DFR (AmDFR or Pallida); and C4'GT (AmC4'GT) (Ono *et al.*, 2006); Figures 2 and S1]. Because the coding sequence of the snapdragon anthocyanidin synthase gene (ANS) was not available in databases, ANS was not included in these interaction assays. In these assays, SUC2-AmFNSII-C_{ub}-LexA-VP16 (i.e. FNSII-C_{ub}) and SUC2-AmF3'H-C_{ub}-LexA-VP16 (i.e. F3'H-C_{ub}) were designed to ensure the P450 N-terminal peptides were inserted in membranes. The SUC2 refers to the 19-residue signal peptide of *Saccharomyces cerevisiae* invertase, while C_{ub}-LexA-VP16 corresponds to the chimera of the C-terminal half of ubiquitin (C_{ub}) and a transcription factor cassette (LexA-VP16). Putative cytoplasmic flavonoid enzymes (collectively referred to as X) were fused with the N-terminal half of a mutated ubiquitin (N_{ub}G) at their N- or C-termini (i.e. N_{ub}G-X or X-N_{ub}G, respectively), and assayed for their interactions with FNSII-C_{ub} and F3'H-C_{ub}. The assay results using the FNSII-C_{ub}/N_{ub}G-X and F3'H-C_{ub}/N_{ub}G-X systems are presented in Figure 2b and c, respectively. Yeast growth on selection medium lacking histidine and adenine, but supplemented with 3-aminotriazole (3AT, which is a competitive metabolic inhibitor of histidine biosynthesis that increases the selection stringency), and the expressed β-galactosidase activities suggested binary protein–protein interactions occurred between FNSII and CHI (Figure 2b), between FNSII and DFR (Figure 2b), and between F3'H and CHI (Figure 2c). A weak interaction between FNSII and CHS was also implied, as the expressed β-galactosidase activity was significantly higher than that observed in the negative control (Figure 2b).

The results for the SU systems using X-N_{ub}G (instead of N_{ub}G-X) in the interaction assays were not necessarily the same as those of the corresponding assays using N_{ub}G-X (Figure S1). For example, for the FNSII/CHI pair, an appreciable level of protein–protein interaction was consistently identified irrespective of the location of the N_{ub}G tag in the CHI fusion (i.e. N_{ub}G-CHI or CHI-N_{ub}G) when SU assays were conducted with FNSII-C_{ub} (Figures 2b and S1b). However, for the FNSII/DFR pair, a protein–protein interaction was detected with the FNSII-C_{ub}/N_{ub}G-DFR system (Figure 2b), but was not clearly detected with FNSII-C_{ub}/DFR-N_{ub}G (Figure S1b). This might be, at least in part, related to the location of the N- and C-termini in the 3D structures

of the enzymes used in the interaction assays. Specifically, the CHI N- and C-termini are positioned close to each other (Jez *et al.*, 2000), hence the N_{ub}G and C_{ub} moieties could be spatially close to each other in the FNSII-C_{ub}/N_{ub}G-CHI and FNSII-C_{ub}/CHI-N_{ub}G systems. By contrast, the DFR N- and C-termini are far from each other (Petit *et al.*, 2007), the interaction assay systems (FNSII-C_{ub}/N_{ub}G-DFR versus FNSII-C_{ub}/DFR-N_{ub}G) could give different results. For the F3'H/CHI pair, however, a protein–protein interaction was identified in the assay with the F3'H-C_{ub}/N_{ub}G-CHI system (Figure 2c), but not with the F3'H-C_{ub}/CHI-N_{ub}G system (Figure S1c), which was in contrast to the results for the FNSII/CHI pair. This implies that the close proximity of N- and C-termini in the protein 3D structure might be a prerequisite, but is insufficient for producing the same results in the SU assays with X-N_{ub}G and N_{ub}G-X. The results might also depend on the structures of the partner proteins in the assay (e.g. FNSII and F3'H).

We also examined all possible combinations of binary interactions among the putative cytoplasmic enzymes with the SU system (Figure 2d for some examples) and yeast two-hybrid (Y2H) assays (Chien *et al.*, 1991; Figure S2; Table S1a for a summary). In the SU analysis, CHI and DFR interacted with each other in the CHI-C_{ub}/N_{ub}G-DFR system (Figure 2d). A weak interaction between CHI and CHS was also implied in the CHI-C_{ub}/N_{ub}G-CHS system, based on yeast growth and the fact the expressed β-galactosidase activity was significantly higher than in the negative control (Figure 2d). However, no appreciable yeast growth was detected with the CHI/DFR, DFR/CHI, CHI/CHS and CHS/CHI systems under the Y2H assay conditions (Figure S2). These results were probably due to the lower sensitivity of the Y2H assay compared with the SU assay. No appreciable yeast growth was detected with any other combination of cytoplasmic flavonoid enzymes in the SU and Y2H assays (Figure S2; Table S1a for a summary).

We then examined whether the binding of DFR to FNSII was inhibited by CHI by using the FNSII-C_{ub}/N_{ub}G-DFR and FNSII-C_{ub}/N_{ub}G-CHI systems in the presence and absence of CHI (or DFR) that was co-expressed in yeast cells under the control of the PGK1 promoter (Figure 3). Although we identified minor interactions between FNSII and CHS and between CHS and CHI in the SU assays, we excluded CHS from these analyses because the interaction signals were too weak.

When FNSII-C_{ub} and N_{ub}G-DFR were co-expressed with DFR (Figure 3a, entry 12), yeast growth (indicative of the interaction between FNSII-C_{ub} and N_{ub}G-DFR) was slightly weaker than that observed in the absence of DFR (entry 4). This suggested that the binding of N_{ub}G-DFR to FNSII-C_{ub} was competitively inhibited by the co-expressed DFR, which was considerably more abundant than N_{ub}G-DFR in yeast cells (Figure 3b, lane 12). When FNSII-C_{ub} and N_{ub}G-DFR were co-expressed with an excess amount of CHI

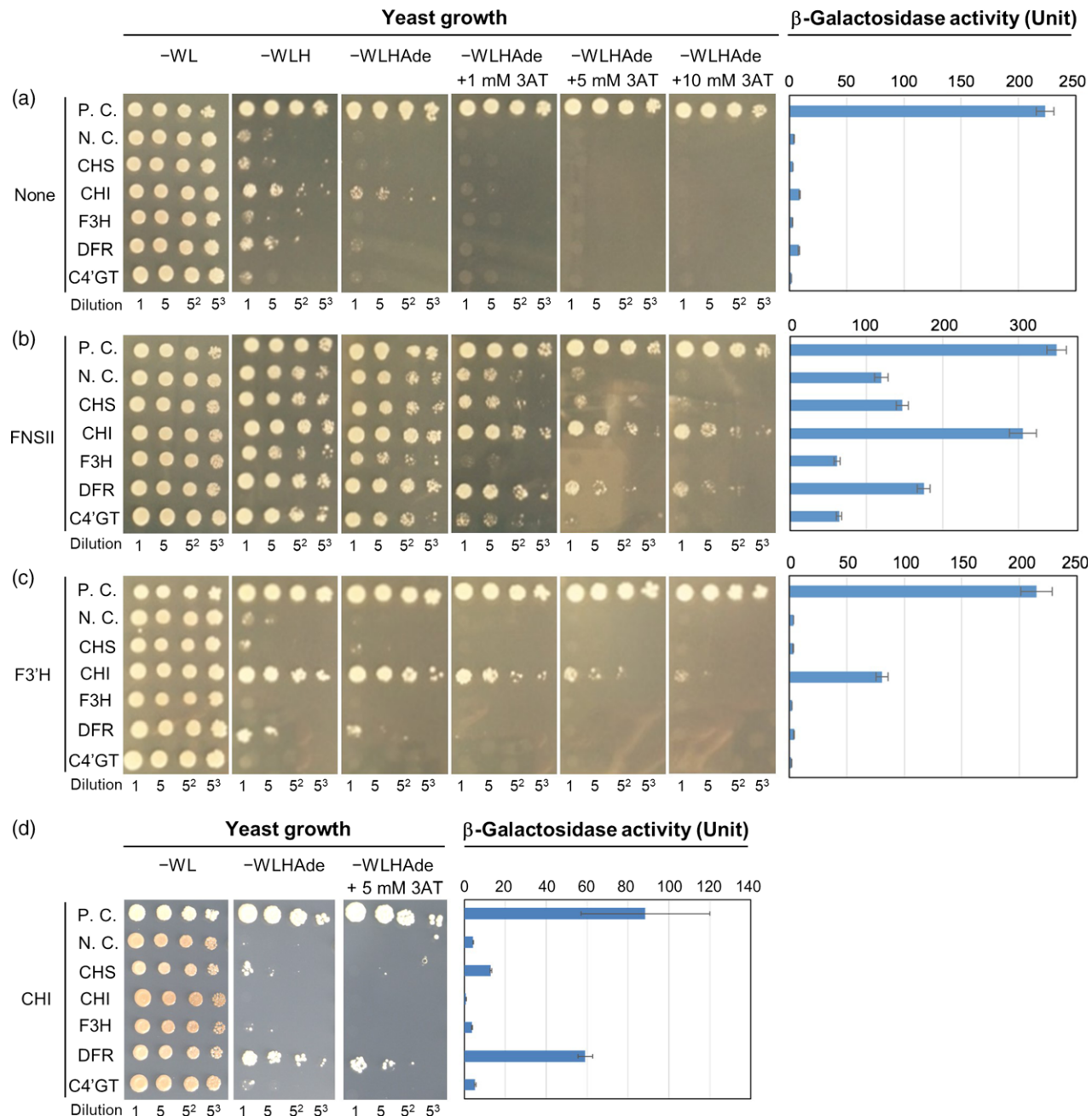


Figure 2. Interactions among snapdragon flavonoid biosynthesis enzymes as determined in the split-ubiquitin (SU) system. The growth of yeast cells co-expressing N_{ub} G-X with (a) C_{ub} -LexA-VP16, (b) AmFNSII- C_{ub} , (c) AmF3'H- C_{ub} or (d) CHI- C_{ub} , where X is CHS, CHI, F3H, DFR or C4'GT, is presented with β -galactosidase activities of transformed cells. Values represent the average of three independent experiments \pm standard deviation. In each panel, P.C. refers to the positive control [transformed cells harboring pOst1- N_{ub}] (a plasmid expressing a fusion protein comprising the yeast resident endoplasmic reticulum (ER) protein Ost1 and the wild-type N_{ub} portion of yeast ubiquitin) and derivatives of pBT3-SUC; N.C. refers to the negative control (transformed cells harboring the empty pPR3-N vector and derivatives of pBT3-SUC). Abbreviated growth media names are as follows: -WL, SD agar medium lacking tryptophan and leucine; -WLH, -WL medium lacking histidine; -WLHAdE, -WLH medium lacking adenine. Additionally, -WLHAdE+1 mM 3AT, for example, refers to the -WLHAdE medium supplemented with 1 mM 3-aminotriazole. CHS, chalcone synthase; CHI, chalcone isomerase; F3H, flavonoid 3-hydroxylase; DFR, dihydroflavonol 4-reductase; C4'GT, chalcone 4'-glucosyltransferase. [Colour figure can be viewed at wileyonlinelibrary.com].

(Figure 3a, entry 8; Figure 3b, lane 8), yeast growth was enhanced compared with that observed in the absence of CHI (entry 4). Moreover, the presence of an excess of DFR (Figure 3b, lane 11) did not inhibit the binding of CHI to

FNSII (entry 3 versus entry 11). The control experiments (entry 3 versus entry 7) did not clearly show yeast growth inhibition probably because the co-expressed CHI was not considerably more abundant than N_{ub} G-CHI in the yeast

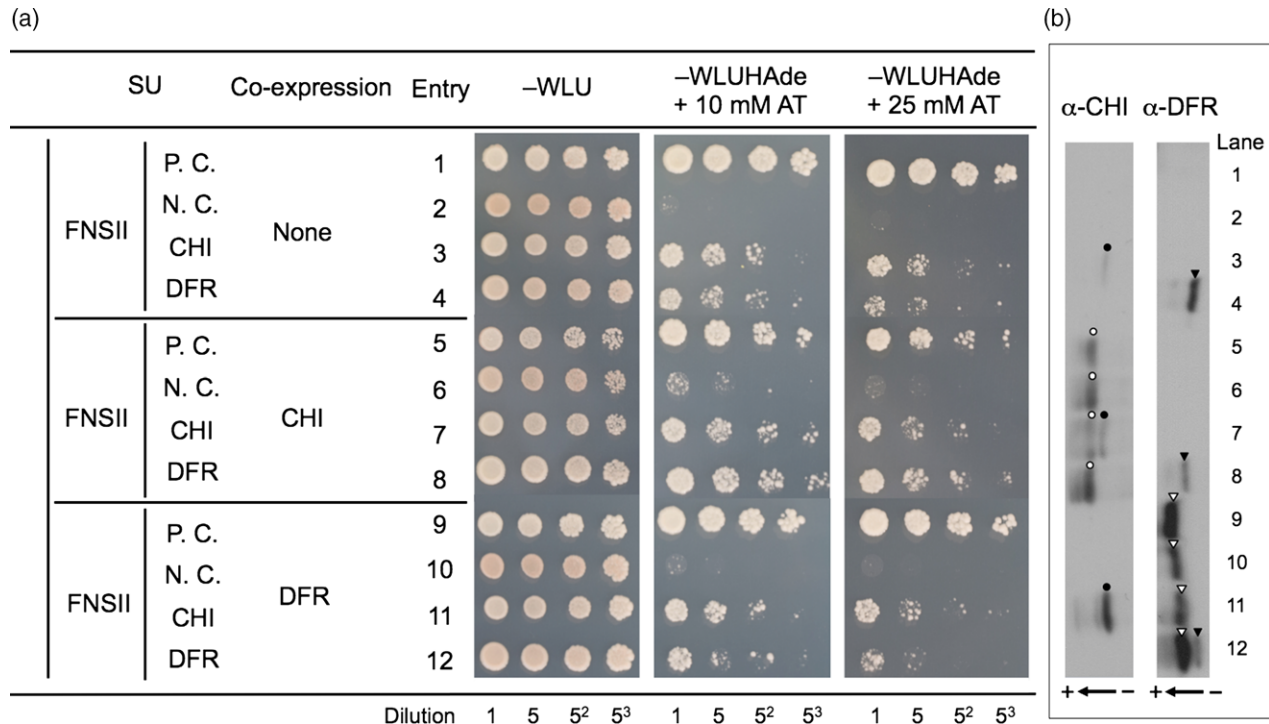


Figure 3. Competitive interaction assays of snapdragon flavone synthase II (FNSII) with chalcone isomerase (CHI) or dihydroflavonol 4-reductase (DFR) in the split-ubiquitin (SU) system.

(a) Entries 3, 7 and 11 present the growth of yeast cells co-expressing FNSII-C_{ub} with N_{ub}G-CHI in the absence of co-expressed CHI and DFR (entry 3), in the presence of co-expressed CHI (entry 7), and in the presence of co-expressed DFR (entry 11). Entries 4, 8 and 12 present the growth of yeast cells co-expressing FNSII-C_{ub} with N_{ub}G-DFR in the absence of co-expressed CHI and DFR (entry 4), in the presence of co-expressed CHI (entry 8), and in the presence of co-expressed DFR (entry 12). Entries 1, 5 and 9 are positive controls, while entries 2, 6 and 10 are negative controls (see Figure 2 legend for details). Abbreviated growth media names are as follows: -WLU, SD agar medium lacking tryptophan, leucine and uracil; -WLUHAd+10 or 25 mM AT, -WLU medium lacking histidine and adenine, but supplemented with 10 or 25 mM 3-aminotriazole. (b) The presence of CHI, N_{ub}G-CHI, DFR and N_{ub}G-DFR in yeast cells was confirmed by an immunoblot analysis. Open and closed circles indicate immuno-positive bands of CHI (24.1 kDa) and N_{ub}G-CHI (31.1 kDa), respectively, while open and closed triangles indicate immuno-positive bands of DFR (49.6 kDa) and N_{ub}G-DFR (56.1 kDa), respectively. Arrows with ± signs indicate the direction of electrophoresis. [Colour figure can be viewed at wileyonlinelibrary.com].

cells (Figure 3b, lane 7). These results suggested that the presence of CHI did not interfere with the interaction between FNSII and DFR. Likewise, the presence of DFR did not interfere with the interaction between FNSII and CHI. Thus, the binding of CHI and DFR to FNSII was not mutually exclusive.

In planta analysis of binary protein–protein interactions between snapdragon flavonoid enzymes

The binary protein–protein interactions with snapdragon flavonoid enzymes were further examined *in planta* by bimolecular fluorescence complementation (BiFC; Ghosh *et al.*, 2000). For these assays, the binary vector pDOE-05 (Gookin and Assmann, 2014) was used to express the proteins of interest, which were each fused in-frame with the N-terminal (residues 1–210) and C-terminal (residues 211–238) fragments (i.e. NmVen210 and CVen210, respectively) of the mVenus protein (mVen, a spectral variant of the green fluorescent protein). The ER structures in cells were visualized via the expression of a derivative of the mCherry

protein with a C-terminal ER-retention signal sequence (HDEL; Nelson *et al.*, 2007).

When AmCHI–NmVen210 was co-expressed with AmFNSII–CVen210 in *benthamiana* tobacco cells (Figure 4a–e; see Figure S3 for the negative controls), the transformed cells produced fluorescence signals (Figure 4b), indicating that FNSII and CHI interacted with each other *in planta*. Moreover, these BiFC signals merged with the fluorescence signals from the ER marker [Figure 4c–e (magnified view)], suggesting that CHI interacted with FNSII on the ER, which is where FNSII is located. Additionally, the co-expression of AmDFR–NmVen210 and AmFNSII–CVen210 yielded BiFC signals in the cells (Figure 4g), which also merged with the fluorescence signals of the ER marker [Figure 4h–j (magnified view)]. Meanwhile, CHI and DFR interacted with each other when AmCHI–NmVen210 and AmDFR–CVen210 were co-expressed (Figure 4l). However, the BiFC signals, which were likely located in the cytoplasm, did not merge with the fluorescence signals of the ER marker [Figure 4m–o (magnified view)]. The SU assay results

suggested there were minor interactions between FNSII and CHS and between CHS and CHI (Figure 2b and d). These observations were consistent with the detection of appreciable BiFC signals when AmCHS–NmVen210 was co-expressed with AmFNSII–CVen210 (Figure 4p–t), and AmCHS–CVen210 was co-expressed with AmCHI–NmVen210 (Figure 4u–y).

Subcellular localization and membrane association analyses of snapdragon flavonoid enzymes

The subcellular localization of snapdragon flavonoid enzymes (FNSII, CHS, CHI, F3H and DFR) was examined by

analyzing the intracellular localization patterns of fluorescence from their chimeric proteins with a spectral variant of GFP [mTurquoise2 (mTq2) or mVen] in *Nicotiana benthamiana* tobacco cells (Figure 5). The ER structures in the cells were visualized via the expression of a derivative of the mCherry protein (Figure 5b). The cytoplasmic space and nucleus of the cells were visualized via the expression of free mVen (Figure 5e, h, k and n). The fluorescence signals of the chimeric AmFNSII–mVen exhibited a sharp network-like pattern in tobacco leaf cells (Figure 5a). Most of the signals merged with the fluorescence signals of the ER marker (Figure 5b and c). The fluorescence signals of

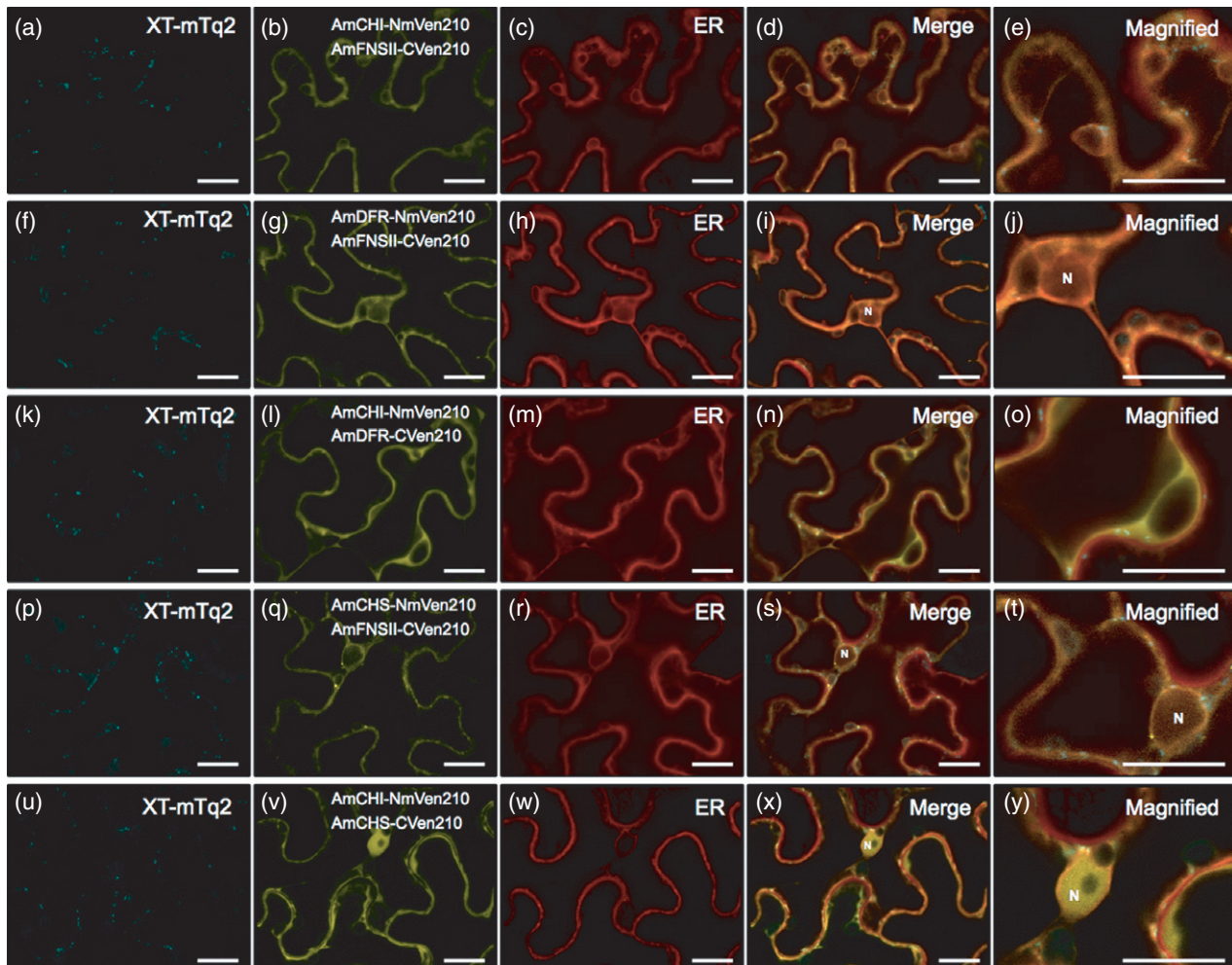


Figure 4. Detection of binary interactions among snapdragon flavonoid enzymes in *Nicotiana benthamiana* tobacco leaf cells by bimolecular fluorescence complementation (BiFC).

Binary interactions between chalcone isomerase (CHI) and flavone synthase II (FNSII) (a–e), between dihydroflavonol 4-reductase (DFR) and FNSII (f–j), between CHI and DFR (k–o), between chalcone synthase (CHS) and FNSII (p–t), and between CHI and CHS (u–y) were analyzed. In each analysis, transformed cells were identified based on XT-mTq2 fluorescence (a, f, k, p and u), and endoplasmic reticulum (ER) structures were identified based on the red fluorescence of an ER marker (c, h, m, r and w). (b) Co-expression of AmCHI-NmVen210 and AmFNSII-CVen210. (g) Co-expression of AmDFR-NmVen210 and AmFNSII-CVen210. (l) Co-expression of AmCHI-NmVen210 and AmDFR-CVen210. (q) Co-expression of AmCHS-NmVen210 and AmFNSII-CVen210. (v) Co-expression of AmCHI-NmVen210 and AmCHS-CVen210. (d) The merged images for (a), (b) and (c). A portion of the merged image is magnified in (e). (i) The merged images for (f), (g) and (h). A portion of the merged image is magnified in (j). (n) The merged images for (k), (l) and (m). A portion of the merged image is magnified in (o). (s) The merged images of (p), (q) and (r). A portion of the merged image is magnified in (t). (x) The merged images of (u), (v) and (w). A portion of the merged image is magnified in (y). Nucleus is indicated by 'N'. Scale bars: 40 µm.

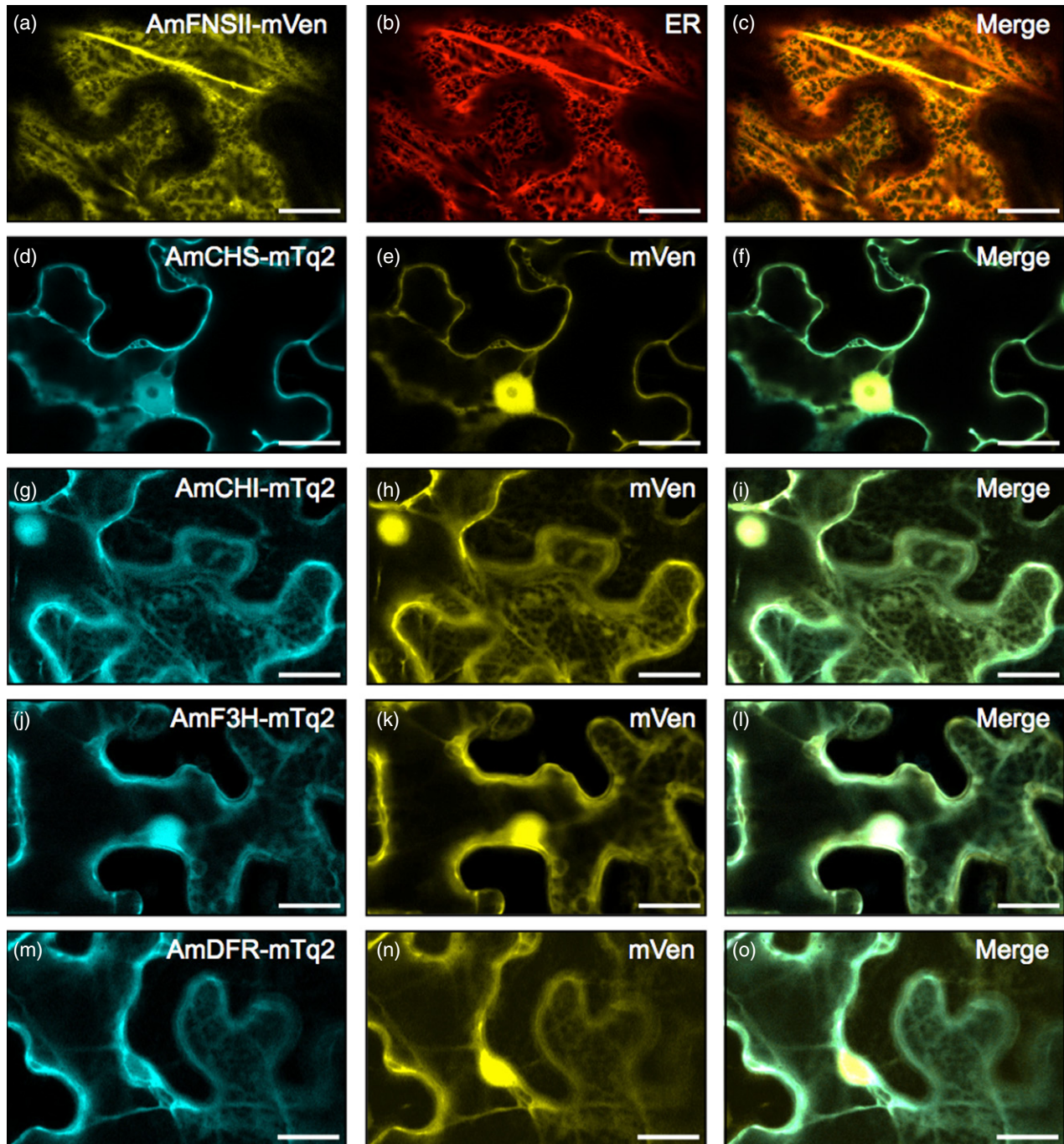


Figure 5. Subcellular localization of some snapdragon flavonoid enzymes as determined by the transient expression of their fluorescence-protein chimeras in *Nicotiana benthamiana* tobacco leaf cells.

Intracellular fluorescence within a single focal plane in leaf cells was observed by confocal laser fluorescence microscopy. (a–c) Co-expression of AmFNSII-mVen and the mCherry derivative with an endoplasmic reticulum (ER) retention signal sequence. (d–f) Co-expression of AmCHS-mTq2 and mVen. (g–i) Co-expression of AmCHI-mTq2 and mVen. (j–l) Co-expression of AmF3H-mTq2 and mVen. (m–o) Co-expression of AmDFR-mTq2 and mVen. (d, g, j and m) Detection of fluorescence from protein chimeras with mTq2. (e, h, k and n) Detection of fluorescence from free mVen. (f) Merged images of (d) and (e). (i) Merged images of (g) and (h). (l) Merged images of (j) and (k). (o) Merged images of (m) and (n). Scale bars: 20 μ m.

AmCHS-mTq2, AmCHI-mTq2 and AmF3H-mTq2 exhibited cloudy distribution patterns in the cytoplasm and nucleus (Figure 5d, g and j), like that of free mVen (Figure 5e, h

and k). Meanwhile, the AmDFR-mTq2 fluorescence signals were detected in the cytoplasm and at the periphery of the nucleus (i.e. the outline of the nucleus; Figure 5m).

We then used immunological methods to examine whether flavonoid enzymes were associated with the membrane of snapdragon petal cells. Specific anti-AmFN-SII epitope antibodies, anti-AmCHS antibodies, anti-AmCHI antibodies and anti-AmDFR epitope antibodies were prepared (we failed to prepare AmF3H-specific antibodies). Crude protein extracts from the petals of snapdragon cultivars that produced different colored flowers (Snapshot Red and Snapshot Yellow) were fractionated by differential centrifugation to obtain soluble and insoluble/microsomal fractions. These protein fractions were then subjected to immunoblot analyses using the antibodies mentioned above. Only petals from stages 1–4 could be used for these analyses. This was because the proteins in the crude extracts of petals from stages 5 and 6 were proteolytically degraded during fractionation procedures. The degradation could not be fully inhibited by the added proteinase inhibitors. In both cultivars, CHS and CHI were present in the soluble and microsomal fractions of petal cells (Figure 6), with estimated proportions (soluble: microsomal, mol/mol) of 5:1 and 25:3 for CHS in Snapshot Red and Snapshot Yellow, respectively, and 70:1 and 23:1 for CHI in Snapshot Red and Snapshot Yellow, respectively. (Figure 6; Experimental Procedures). Interestingly, DFR was almost exclusively localized in the microsomal fraction, with an estimated proportion (soluble: microsomal, mol/mol) of 3:22 in Snapshot Red. The DFR protein was not detected in Snapshot Yellow, which was consistent with

the fact that the *DFR* gene was not expressed in this anthocyanin-free cultivar. Moreover, the immuno-positive signals for CHS, CHI and DFR in the microsomal fraction did not arise from contamination by the soluble fraction, as revealed by control experiments (Figure S4). Furthermore, a considerable portion of microsome-associated CHS and CHI might have been removed from membranes during the isolation of microsomes because of their potentially weak interactions with microsomes. The FNSII protein was detected exclusively in the insoluble membrane fraction during the first flower development stage (Figure 6), as expected based on the fluorescence image analysis.

Sequential accumulation of flavonoids and sequential expression of flavonoid enzyme genes during snapdragon flower development

To propose a flavonoid metabolon model (see Discussion) based on the results described above, we further examined the temporal flavonoid accumulation patterns in snapdragon petals. Three major snapdragon flavonoids (flavones, anthocyanins and aurones) in the petals of nine different cultivars (i.e. different colors; Figure S5), all of which were *Nivea*⁺ plants, were analyzed by high-performance liquid chromatography (HPLC) during flower development (six stages; Figure 7; Table S2). Flavone glycosides were detected in the petals of all examined cultivars. In the petals of cyanidin (Cy)-accumulating cultivars (i.e. Snapshot Red, Snapshot Red Bicolor and FloralShower Red), Cy

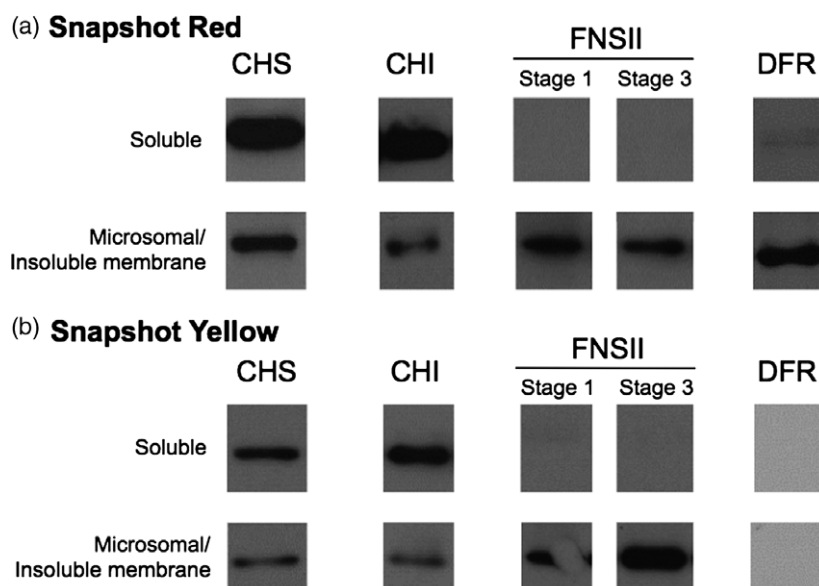


Figure 6. Immunological detection of flavonoid enzymes in soluble and microsomal/membrane fractions from (a) Snapshot Red and (b) Snapshot Yellow petal cells.

For chalcone synthase (CHS), chalcone isomerase (CHI) and dihydroflavonol 4-reductase (DFR), the soluble and microsomal fractions of petal cells (stage 3) were analyzed, and for flavone synthase II (FNSII), soluble and insoluble membrane fractions of petal cells (stages 1 and 3) were analyzed. For further details, see Experimental procedures.

3-O-rutinoside was the exclusive anthocyanin, and the flavones that accumulated were glucuronides of apigenin (Ap), luteolin and chrysoeriol. In the petals of pelargonidin (Pg)-accumulating cultivars (i.e. Snapshot Burgundy, Snapshot Orange and Snapshot Pink), 3-O-rutinoside was the only anthocyanin, and the flavones that accumulated were glucuronides of Ap. Additionally, 6-O-glucosides of aureusidin (Au) and bracteatin (Br) accumulated in all tested cultivars, although there was only a trace amount of Br 6-O-glucosides in the Snapshot White petals.

Our data indicated that flavones began to accumulate during the first flower development stage in all examined snapdragon cultivars, with levels approaching the maximum observed at stages 3–5 (Figure 7a–c, upper panels). In cultivars that produced reddish flowers (i.e. Cy- and Pg-accumulating cultivars), the petals essentially lacked anthocyanins at stage 1. However, the anthocyanins began to accumulate at stages 2–3, with maximum levels at stages 5–6 (Figure 7a and b, middle panels). In the cultivars with reddish and yellow flowers, aurones were not detected in petals at stages 1–4, began to accumulate at stage 5, and reached their maximum levels at stage 6 (Figure 7a–c, lower panels). Thus, in the anthocyanin-accumulating petals, flavones accumulated first, followed by anthocyanins and finally aurones. These sequential flavonoid accumulation patterns were also observed in the petals of white and yellow snapdragon varieties, although anthocyanins were absent because *DFR* was not expressed.

To explain the observed sequential flavonoid accumulation patterns in snapdragon, the temporal expression patterns of genes encoding flavonoid biosynthetic enzymes were analyzed in the petals of four cultivars that produced different colored flowers (Snapshot Red, Snapshot Orange, Snapshot Yellow and Snapshot White). Relative gene expression levels were determined by quantitative real-time-polymerase chain reaction (qRT-PCR; Figure 8). The results were compared with those of flavonoid accumulation. The highest *AmCHS1* (*Nivea*) transcript levels were observed at stages 5–6, depending on the cultivar (*CHS* panels). In contrast, the highest *AmCHI1* transcript levels were detected during the early stages of flower development (stages 1–3; *CHI* panels). The *AmFNSII* transcripts were present at appreciable levels in the petals of all cultivars at stage 1, and were most abundant at stage 3 (Snapshot Red), stage 4 (Snapshot White and Snapshot Yellow), or stage 5 (Snapshot Orange; *FNSII* panels). For the anthocyanin biosynthesis genes, the *AmF3H* transcript levels were higher at the later stages (stages 3–5) of flower development, irrespective of flower color (*F3H* panel). Additionally, *AmDFR* transcripts were present only in the petals of cultivars that produced cyan flowers (i.e. Snapshot Red and Snapshot Orange), and began to accumulate at stage 2 (*DFR* panel). The *AmF3H* (*Eosinea*) transcripts were detected in the petals of the Cy-accumulating cultivar (i.e.

Snapshot Red) at all stages, with maximum levels at stage 5 (*F3H* panel). The highest transcript levels for the aurone biosynthesis genes (*AmC4'GT* and *AmAS1*) were observed at stages 5–6 in the Snapshot Red, Snapshot Orange and Snapshot Yellow petals (*C4'GT* panel and *AS* panel). Meanwhile, very low *AmC4'GT* transcript levels were detected in the Snapshot White petals.

Binary interactions among *torenia* flavonoid enzymes determined using SU and Y2H systems

We examined whether (or how) the networks of binary protein–protein interactions detected for snapdragon flavonoid enzymes were conserved in another closely related plant species. We selected the *torenia* flavonoid enzyme system, because *torenia* is also a lamiales plant that produces flavones and anthocyanins via flavonoid pathways similar to those of snapdragon. Binary interactions among *torenia* flavonoid enzymes [i.e. CHS, two isozymes of type-1 CHI (*CHI1_1* and *CHI1_2*; Fujino *et al.*, 2014), FNSII (Akashi *et al.*, 1999; Ueyama *et al.*, 2002), F3H, DFR, ANS, F3'H (Ueyama *et al.*, 2002) and F3'5'H] were comprehensively analyzed using the SU and Y2H systems (Figures 9 and S6). The analyses of yeast growth and β -galactosidase activity in the SU system (Figure 9) revealed FNSII interacted with *CHI1_1*, *CHI1_2*, F3H and DFR (Figure 9a). A relatively weak interaction between FNSII and ANS was also detected (Figure 9a). Additionally, F3'H interacted with *CHI1_1* and *CHI1_2* (Figure 9b). Neither yeast growth nor β -galactosidase activity was detected when binary interactions between F3'5'H and cytoplasmic enzymes were assayed (Figure 9c). The data also indicated interactions between DFR and *CHI1_1*, and between DFR and F3H (Figure 9d). The observed physical interaction partnerships between FNSII and CHI, between FNSII and DFR, and between CHI and DFR in the *torenia* system were similar to the observations in the snapdragon system, and were confirmed *in planta* by BiFC assays (Figure 10). We examined all possible combinations of binary interactions among the putative *torenia* cytoplasmic flavonoid enzymes (CHS, CHI, FNSII, F3H, DFR and ANS) using Y2H assays. No appreciable yeast growth was detected with any combination under the Y2H assay conditions (Figure S6), as was the case for the snapdragon flavonoid system (Figure S2).

DISCUSSION

In this study, we analyzed the binary interactions among the flavonoid enzymes of lamiales plants (snapdragon and *torenia*) and clarified their physical interaction partnerships (Figure 11a and b, respectively). We also examined the subcellular localizations and membrane associations of snapdragon flavonoid enzymes, as well as the expression levels of the corresponding genes. Furthermore, we analyzed the flavonoid accumulation patterns in snapdragon. Considered together, our results suggest that an ER-

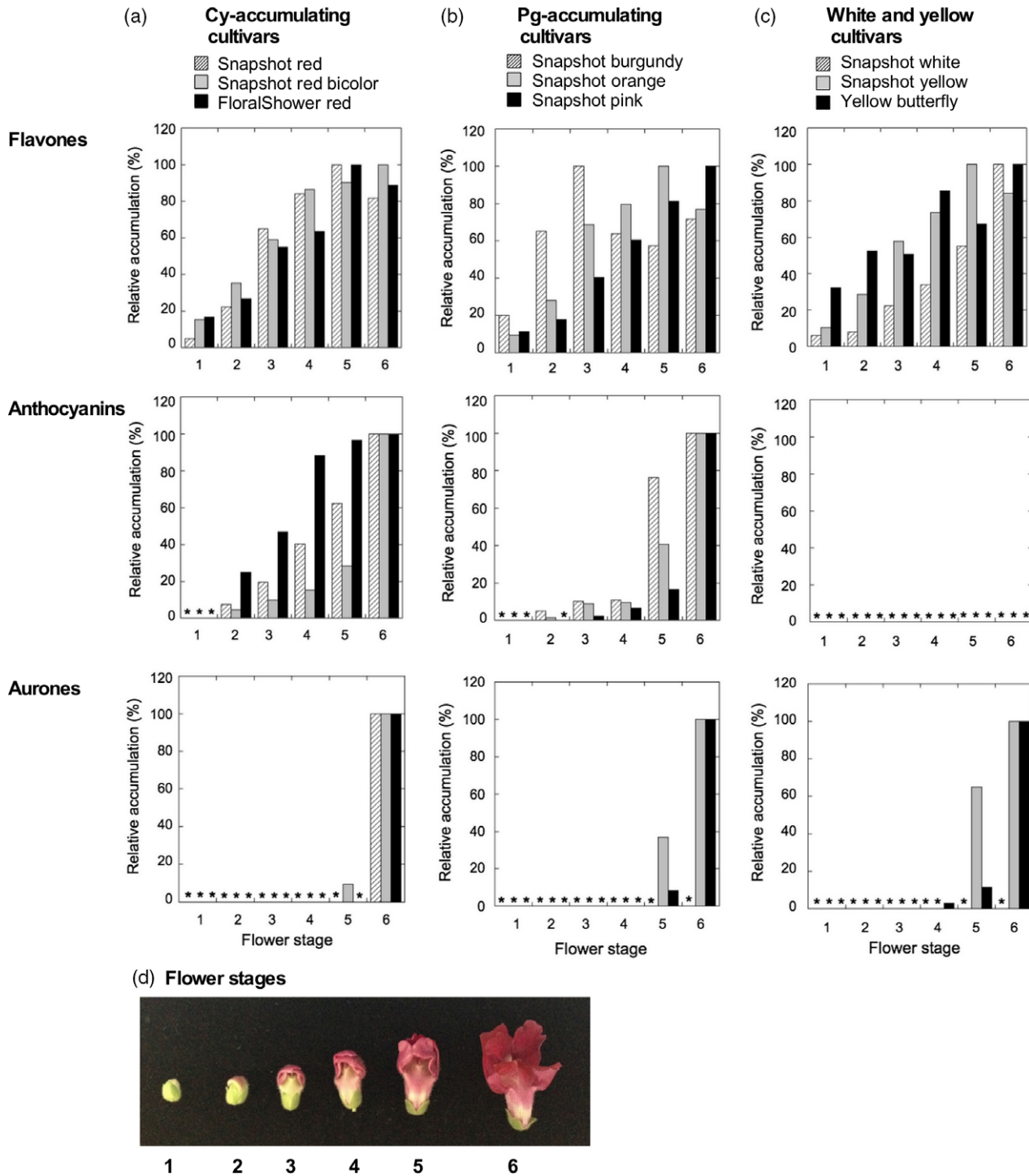


Figure 7. Flavonoid accumulation in the petals of (a) Cy-accumulating, (b) Pg-accumulating, and (c) white and yellow cultivars of snapdragon during flower development.

For each commercial variety, the highest flavonoid content (Table S2) was set as 100%. Flavones were determined as their aglycons after an acid hydrolysis with 1 M HCl at 100°C for 1 h. Anthocyanin contents were determined as their 3-O-rutinosides, while aurone contents were determined as their 6-O-glucosides (Au 6-O-glucoside and Br 6-O-glucoside). (d) Developmental stages of snapdragon flowers. For further experimental details, see Experimental procedures and Table S3. *, not detected.

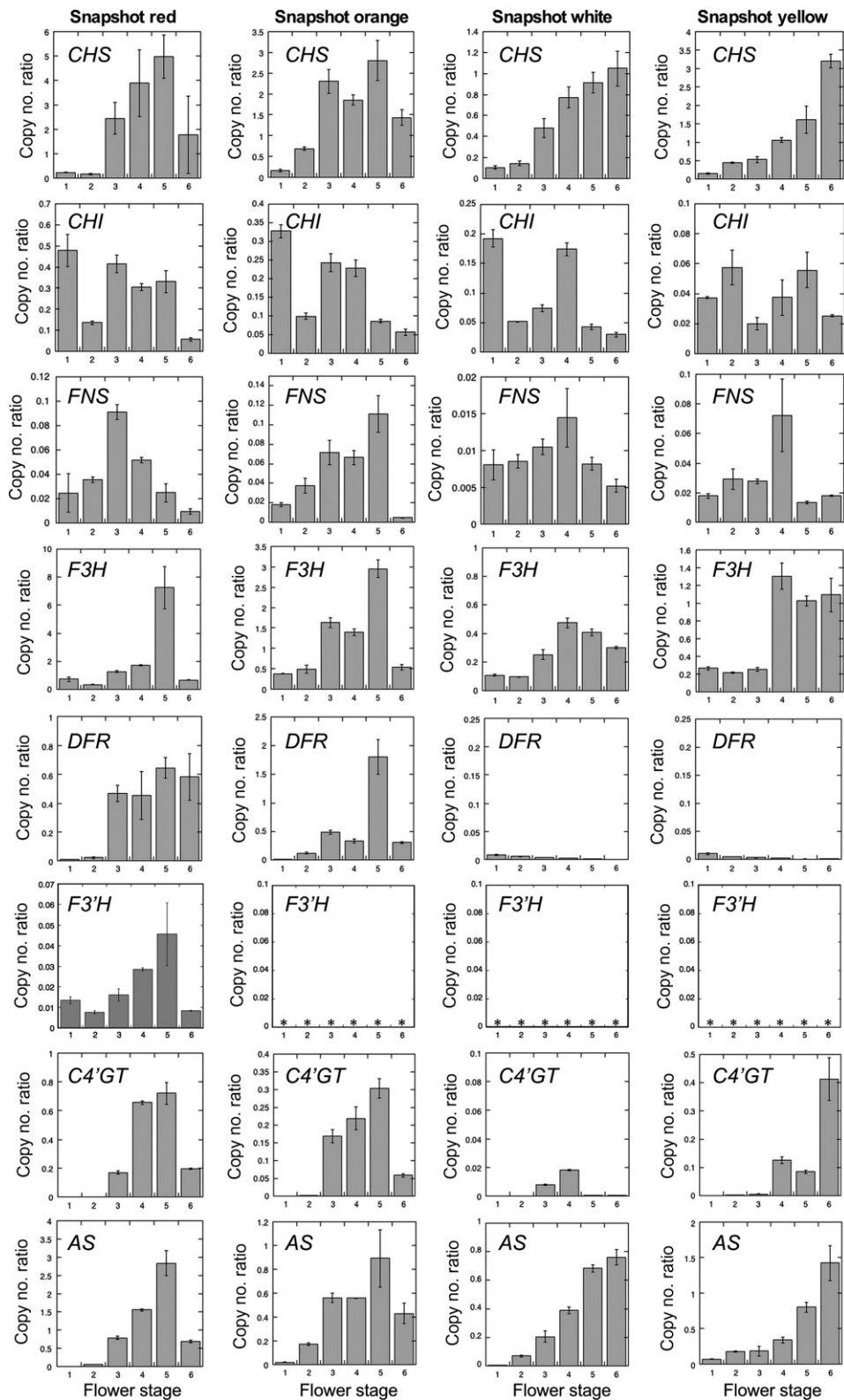
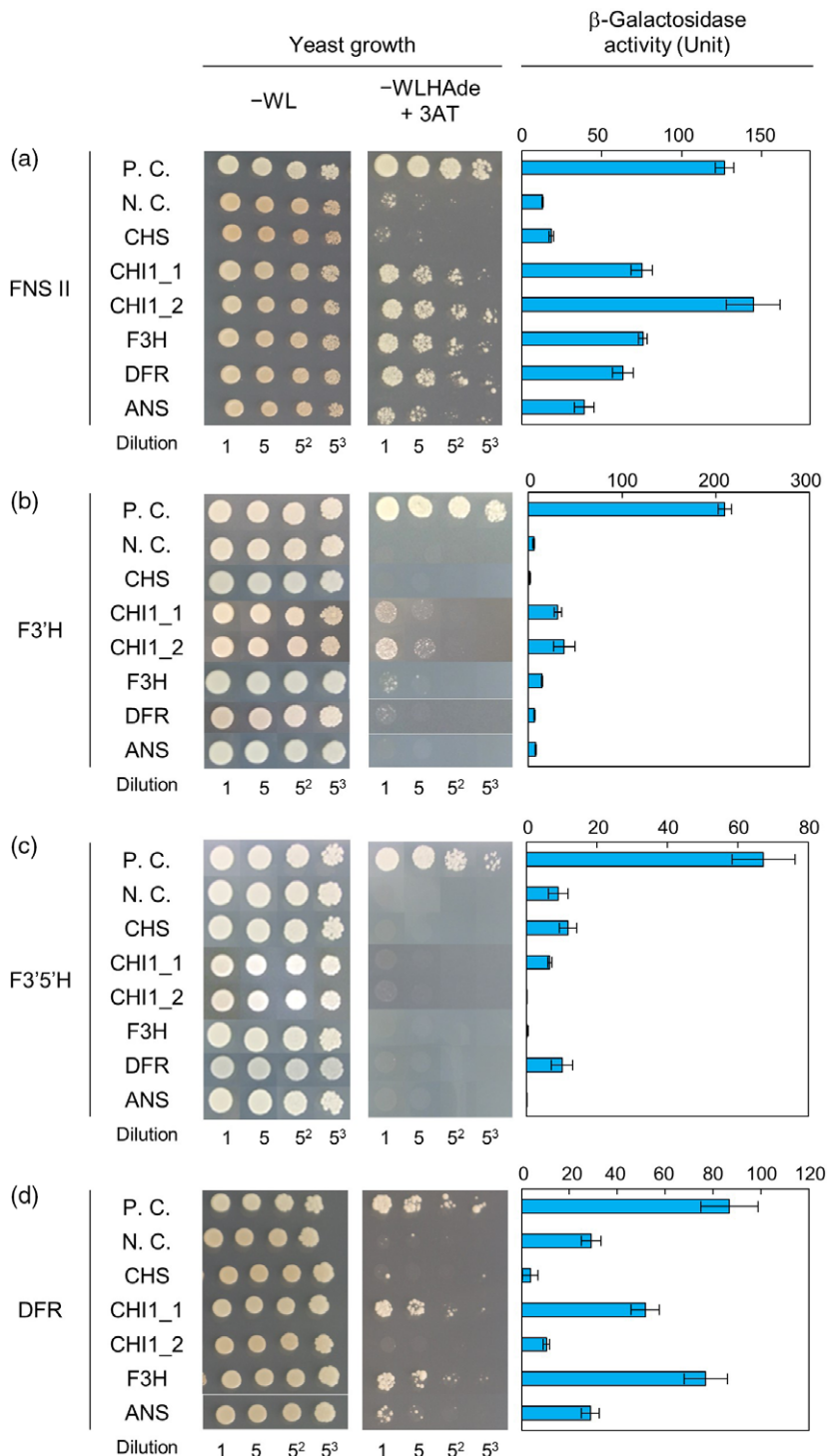


Figure 8. Transcriptional analysis of flavonoid enzyme genes in the petals of different snapdragon cultivars during flower development. Copy number ratios were expressed as values relative to that of the snapdragon ubiquitin gene (*AmUBQ*) (DDBJ/ENA/GenBank accession number, X67957). Values represent the average of three independent experiments \pm standard deviation. For experimental details regarding the quantitative real-time-polymerase chain reaction (qRT-PCR), see Experimental procedures. *, not detected.



localized FNSII serves as a flavonoid metabolon component in the analyzed plants. Our findings provide additional evidence supporting the long-suspected organization of flavonoid enzyme complexes tethered to the ER. Moreover, the data presented herein strongly suggest that the flavonoid enzyme systems in these plants are organized differently from those of *A. thaliana* and soybean.

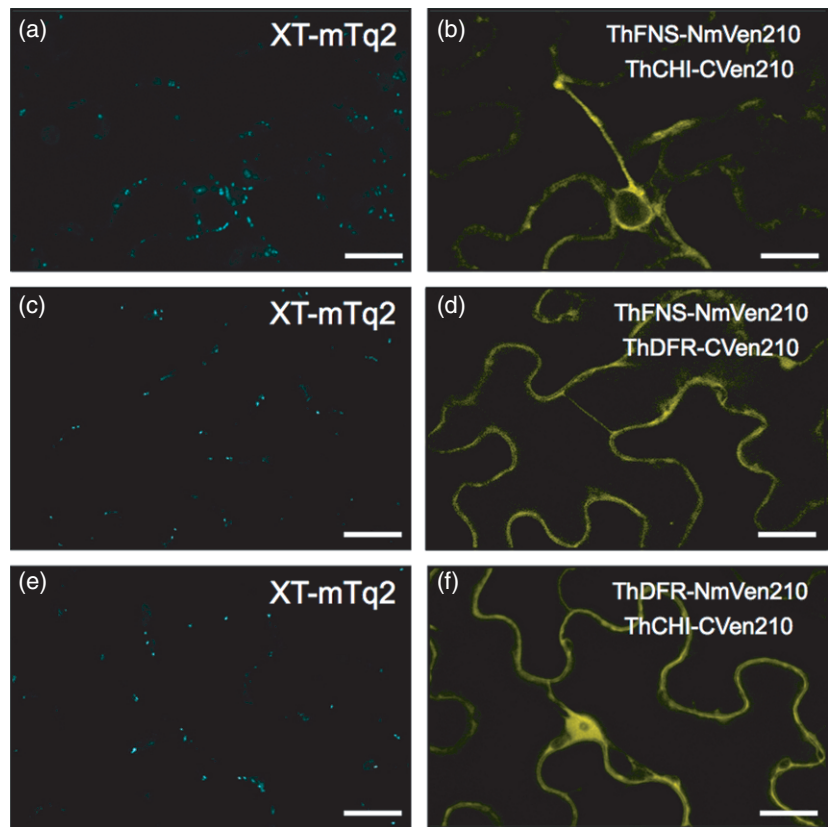
Physical interaction partnerships, subcellular localizations and membrane associations of snapdragon flavonoid enzymes: implications for the occurrence of a flavonoid metabolon in snapdragon

Among the snapdragon flavonoid enzymes examined, the following sets of binary interactions were identified in the

Figure 9. Interactions of *torenia* P450s [flavone synthase II (FNSII), flavonoid 3'-hydroxylase (F3'H) and flavonoid 3',5'-hydroxylase (F3'5'H)] and dihydroflavonol 4-reductase (DFR) with soluble flavonoid enzymes as assayed in the split-ubiquitin (SU) system. Left: growth of yeast cells co-expressing (a) FNSII-C_{ub}, (b) F3'H-C_{ub}, (c) F3'5'H-C_{ub}, and (d) DFR-C_{ub} with N_{ub}G-X, where X is CHS, CHI1_1, CHI1_2, F3H, DFR or anthocyanidin synthase (ANS). Right: β -galactosidase activities of transformed cells. Values represent the average of three independent experiments \pm standard deviations. For details regarding the positive control (P.C.) and negative control (N.C.) as well as the names of the growth media, refer to Figure 2 legend. [Colour figure can be viewed at wileyonlinelibrary.com].

Figure 10. Detection of binary interactions of some torenia flavonoid enzymes in *Nicotiana benthamiana* tobacco leaf cells by bimolecular fluorescence complementation (BiFC).

Binary interactions between flavone synthase II (FNSII) and chalcone isomerase (CHI) (a and b), between FNSII and dihydroflavonol 4-reductase (DFR) (c and d), and between DFR and CHI (e and f) were analyzed. In each analysis, transformed cells were identified based on the XT-mTq2 fluorescence (Golgi marker; a, c and e). (b) Co-expression of ThFNS-NmVen210 and ThCHI-CVen210. (d) Co-expression of ThFNS-NmVen210 and ThDFR-CVen210. (f) Co-expression of ThDFR-NmVen210 and ThCHI-CVen210. Scale bars: 40 µm.



SU system: FNSII/CHS, FNSII/CHI, FNSII/DFR, CHS/CHI, CHI/DFR and F3'H/CHI (Figure 2; Table S1a for a summary). These interactions were further corroborated by the results of BiFC assays (Figures 4 and 11a for a summary), strongly suggesting that these protein–protein interactions indeed occur *in planta*.

An immunoblot analysis revealed that FNSII was present only in the insoluble membrane fraction of snapdragon petal cells (Figure 6). Moreover, when the intracellular localization of FNSII was analyzed by fluorescence imaging of the heterologous AmFNSII-mVen chimera in *N. benthamiana* tobacco leaves, the fluorescence signals showed a network-like pattern, most of which merged with the fluorescence signals from the ER marker (Figure 5). These observations imply that FNSII was localized to the ER and related membrane systems (e.g. ER bodies). In contrast, the fluorescence of each of the mTq2 chimeras with CHI, F3H and DFR exhibited cloudy distribution patterns in the cytoplasm. The mTq2 chimeras of CHI and F3H were also detected in the nuclear interior, while the mTq2 chimera of DFR was found at the periphery of the nucleus (Figure 5). Additionally, a signal sequence for intracellular translocations to specific organelles was not detected in the primary structures of CHI, F3H, DFR and CHS. Thus, these flavonoid enzymes are likely cytosolic proteins. Nonetheless, immunoblot

analyses revealed that CHS and CHI were present in both the soluble and microsomal fractions of snapdragon petal cells, irrespective of flower color, and DFR was found exclusively in the microsomal fraction of Snapshot Red petal cells (Figure 6). The observed membrane association of CHS, CHI and DFR was consistent with the fact that these flavonoid enzymes were able to interact with ER-localized FNSII. The exclusive localization of DFR in the microsomal fraction of Snapshot Red petal cells may be due to the potentially strong interaction between DFR and the DFR-binding proteins on the ER membrane (i.e. FNSII and FNSII-bound CHI). The DFR-binding proteins are more abundant than DFR in petal cells during the first flower development stage. Because CHS, CHI and FNSII are consecutive enzymes in the snapdragon flavonoid pathway (Figure 1), it is likely that these binary interactions produce a metabolon that facilitates flavone synthesis in the petal cells. This metabolon may form via a mechanism such as ‘micro-compartmentalization’ of the metabolic pathway or ‘metabolite channeling’. Thus, a membrane-bound ‘flavone metabolon’ containing CHS, CHI and FNSII has been proposed (Figure 12a). Moreover, F3'H/CHI may also represent a consecutive pair of enzymes in the flavonoid pathway. Thus, it is likely that this binary interaction also produces a metabolon for the efficient synthesis of 3'-hydroxyflavonoids.

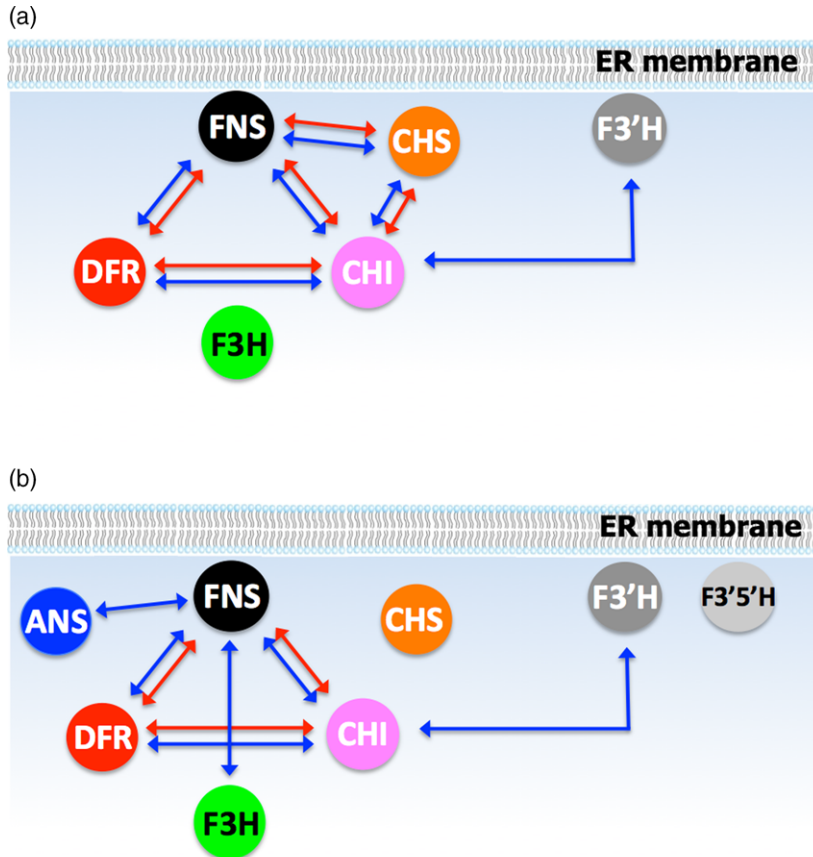


Figure 11. Schematic representations of flavonoid metabolon models in (a) snapdragon and (b) torenia.

Colored circles indicate flavonoid biosynthesis enzymes (refer to Figure 1 legend for abbreviated enzyme names). Blue double-headed arrows indicate protein–protein interactions identified in the yeast systems [split-ubiquitin (SU) and yeast two-hybrid (Y2H) systems], while red double-headed arrows indicate protein–protein interactions confirmed in plant systems [bimolecular fluorescence complementation (BiFC)].

We identified physical interaction partnerships between DFR and FNSII, and between DFR and CHI (Figure 11a). We also observed that DFR and CHI interacted with FNSII in a non-exclusive manner (Figure 3). Additionally, DFR/FNSII and DFR/CHI are non-consecutive pairs of enzymes in the pathway (Figure 1). The activities of FNSII and DFR are specifically required for the formation of flavones and anthocyanins, respectively, which are different classes of flavonoids. These observations raise the possibility that, during anthocyanin biosynthesis in snapdragon, FNSII plays a structural (but not catalytic) role as a hub to which CHS, CHI and DFR (and probably other soluble enzymes) are tethered to form an ‘anthocyanin metabolon’ (Figure 12b). Among the snapdragon flavonoid enzymes available for the binary interaction assays, we failed to identify the binding of F3H to FNSII, F3'H or other soluble flavonoid enzymes. The involvement of this enzyme in the metabolon may require pre-existing complexes of other biosynthetic enzymes, including P450s or an accessory protein(s).

To examine the possible role of FNSII in the formation of an anthocyanin metabolon in snapdragon, we examined whether suppressing *FNSII* expression in snapdragon flowers would decrease anthocyanin accumulation in the petals. Unfortunately, all of our attempts to suppress *FNSII*

expression in snapdragon, including virus-induced gene silencing and RNAi via peptide-based gene delivery, were unsuccessful. However, the temporal patterns of flavonoid accumulation and flavonoid enzyme expression during Snapshot Red flower development appeared to be consistent with the proposed role of FNSII in snapdragon anthocyanin biosynthesis. Anthocyanin biosynthesis genes encoding enzymes further down the pathway (*F3H*, *DFR* and *ANS*; Figure 1) are reportedly expressed in a coordinated manner during the late stages of flower development (Martin *et al.*, 1991; Jackson *et al.*, 1992; Schwinn *et al.*, 2006), and follow the expression of *CHI*. Therefore, these late-stage biosynthesis genes appear to share a common regulatory mechanism. This differential regulation of ‘early’ and ‘late’ flavonoid genes is a common feature among plants, with the specific mechanisms having been characterized in several species, including *A. thaliana* and petunia (Winkel-Shirley, 2001). Our proposal that FNSII is a component of an anthocyanin metabolon in snapdragon implies that FNSII should be expressed before the flavonoid enzymes involved in the late stage of anthocyanin biosynthesis (e.g. DFR) to enable the anthocyanin metabolon to form. As expected, FNSII was highly abundant in the insoluble membrane fraction of petal cells during the first

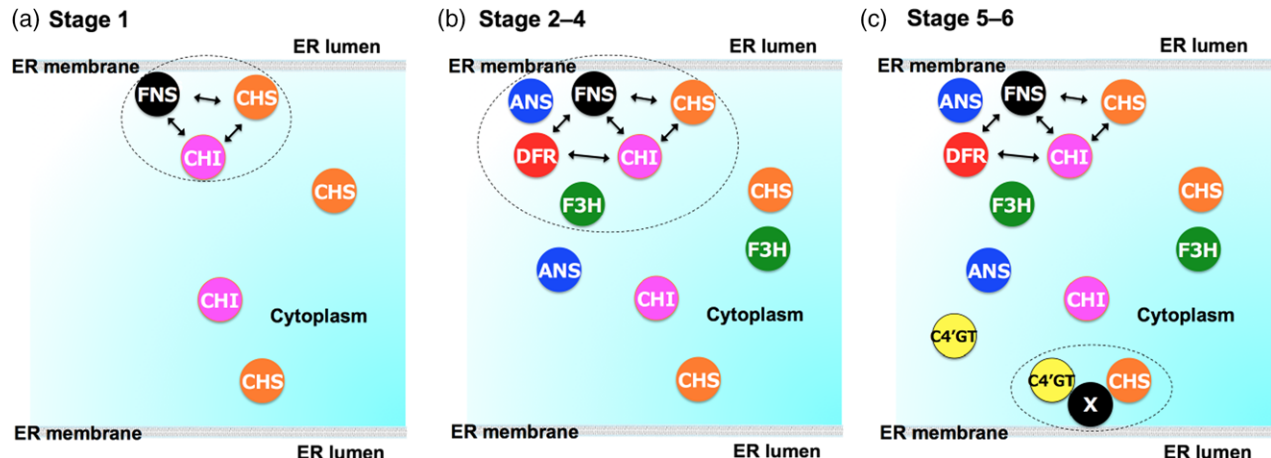


Figure 12. Proposed metabolon model considering the temporal flavonoid accumulation patterns in the snapdragon petal cells used in this study. (a) Stage 1 of flower development. (b) Stages 2–4. (c) Stages 5–6. Colored circles indicate flavonoid enzymes, and dashed circles indicate proposed metabolons. See also legend to Figure 1 for abbreviations of enzyme names. Double-headed arrows show protein–protein interactions identified in this study. X, unknown protein. Note that the protein–protein interactions and gene expression levels of anthocyanidin synthase (ANS) were not examined in this study.

snapdragon flower development stage (Figure 6). Moreover, flavones were always present in the Pg- and Cy-accumulating petals (Figure 7). Three major snapdragon flavonoids (flavones, anthocyanins and aurones) exhibited a sequential accumulation pattern in the Pg- and Cy-accumulating cultivars examined in this study. Specifically, flavone glycosides accumulated first (stage 1), followed by anthocyanins (at stages 2–3), and finally aurone glucosides (stages 5–6). This pigmentation pattern has been generally observed in other snapdragon cultivars. For example, analyses of the flavonoid composition in the petals of 60 different snapdragon cultivars and strains (i.e. different colors) revealed that all but three *nivea*⁺ cultivars with white flowers accumulated flavone glycosides, whose accumulation preceded those of the anthocyanins and aurones (Toki, 1988). The sequential pattern of flavonoid accumulation was consistent with the transcriptional patterns of snapdragon flavonoid enzyme genes during flower development. Our results also indicated that *CHI* and *FNSII* were expressed first (from stage 1; Figure 8), followed by flavonoid enzyme genes involved in the later steps of anthocyanin biosynthesis (*F3H* and *DFR*; from stages 2 to 5), and finally genes involved in aurone biosynthesis (*C4'GT* and *AS*; from stages 3 to 5). Thus, how flavonoid enzyme molecules are organized in snapdragon petal cells and regulated to produce three major flavonoids is illustrated in Figure 12a–c. The formation of an ‘aurone biosynthetic metabolon’ (Figure 12c), if it occurs at all, might not be mediated by *FNSII* and other enzymes involved in anthocyanin biosynthesis. The validity of the model, along with the possible structural role of *FNSII* during anthocyanin biosynthesis, will need to be investigated in future studies.

In Snapshot Red, Snapshot Orange and Snapshot Yellow petal cells, *C4'GT*, which is a key enzyme in the

snapdragon flavonoid pathway for aurone biosynthesis in petal cells, is finally expressed along with the vacuolar aureusidin synthase (Nakayama *et al.*, 2000; Ono *et al.*, 2006) to establish the aurone biosynthesis pathway. However, we did not detect any interaction between *C4'GT* and the flavonoid enzymes in the SU and Y2H assays. These results suggest that an ‘aurone biosynthesis metabolon’, if it occurs at all, might not include *FNSII* and other flavonoid enzymes involved in anthocyanin biosynthesis.

Physical interaction partnerships in *torenia*: similarities to snapdragon networks and implications for their functional significance

Comprehensive analyses of binary protein–protein interactions using the SU and Y2H systems and BiFC assays revealed that, in *torenia*, *FNSII* interacted with *CHI* isozymes and other anthocyanin biosynthesis enzymes (*F3H*, *DFR* and *ANS*; Figures 9 and 10), and *F3'H* interacted with *CHI* isozymes (Figure 9b; Table S1b for a summary). A *CHI* isozyme (*CHI1_1*) also interacted with *DFR* (Figure 9d). We did not detect any binary interactions between *F3'5'H*, which is not active in snapdragon, and other tested *torenia* flavonoid enzymes (Figure 9c). Other proteins (e.g. P450s) might be needed for *F3'5'H* to interact with other *torenia* flavonoid enzymes. The similarities in the interaction networks of flavonoid enzymes involving *FNSII* in *torenia* and snapdragon (Figure 11) were consistent with the close phylogenetic relationship between these plants. In this context, it is important to note that the effects of the co-suppression of *FNSII* expression on anthocyanin contents in *torenia* flowers have been examined (Ueyama *et al.*, 2002). The results of this previous study strongly support the importance of *FNSII* in anthocyanin biosynthesis in *torenia* petal cells. Specifically, *FNSII* was co-suppressed in

blue-violet torenia flowers in an attempt to engineer flowers with a deeper petal color. This strategy was based on the fact that the biosyntheses of flavones and anthocyanins compete with each other for flavanones as the common precursors (Figure 1). Suppression of *FNSII* expression (i.e. decreased *FNSII* activity) was expected to result in increased anthocyanin accumulation because of increased channeling of flavanones toward anthocyanin production at the expense of flavone formation (Figure 1). This strategy was justified by recent observations of black dahlia, whose black petals are due to the accumulation of large amounts of Cy-based anthocyanins. In black dahlia, *FNSII* expression is suppressed by endogenous post-transcriptional gene silencing, resulting in increased production of anthocyanins with a concomitant decrease in flavone production (Thill *et al.*, 2012; Deguchi *et al.*, 2013). In the above-mentioned torenia system (Ueyama *et al.*, 2002), the co-suppression of *FNSII* expression decreased flavone abundance and increased the amount of flavanones in the petals, as expected. However, contrary to initial expectations, the amount of anthocyanins in the petals of the *FNSII*-suppressed torenia decreased considerably, yielding a relatively pale flower color (Ueyama *et al.*, 2002). The reason for this unexpected result was unknown, but our results suggest that it could be explained by the role of *FNSII* as a component of the metabolon related to anthocyanin production.

In red and black dahlia cultivars, the petal flavone and anthocyanin contents are inversely related to each other (Thill *et al.*, 2012; Deguchi *et al.*, 2013). In contrast, we observed a positive correlation between flavone and anthocyanin contents in cyan snapdragon petals during flower development (Figure S7). These observations also support the proposal that *FNSII* is an important component of the anthocyanin metabolon in snapdragon (Figure 12b). However, further studies are needed to characterize *FNSII* functions related to anthocyanin production in lamiales plant species.

Differences in flavonoid metabolons among plant species

Thus far, the existence of a metabolon for flavonoid biosynthesis has been confirmed in *A. thaliana*, which is a Brassicales plant that is distantly related to snapdragon and torenia. However, the *A. thaliana* genome lacks the *FNSII* gene. Therefore, the organization of the *A. thaliana* flavonoid metabolon differs from that of the flavonoid metabolons in snapdragon and torenia. In the *A. thaliana* flavonoid metabolon, CHS has structural and catalytic roles, functioning as a hub for the formation of the metabolon and synthesizing the flavonoid precursor (THC), respectively (Winkel-Shirley, 1999; Crosby *et al.*, 2011). Recent reports described a metabolon for isoflavone biosynthesis in soybean (a Fabales plant), where flavonoid enzymes are tethered to the ER via two P450 proteins (2-hydroxyisoflavanone synthase

and cinnamate 4-hydroxylase; Dastmalchi *et al.*, 2016; Waki *et al.*, 2016). In this case, the activities of these P450s were indispensable for isoflavone biosynthesis. Hence, these P450s play both structural and catalytic roles in the soybean isoflavone metabolon. This contrasts with the suggested role of *FNSII* in the proposed anthocyanin metabolons of snapdragon and torenia. Additionally, silencing *FNSII* enhanced anthocyanin production in dahlia (an Asteraceae plant; Thill *et al.*, 2012; Deguchi *et al.*, 2013), but not in torenia. This implies that the formation of the anthocyanin metabolon in dahlia petal cells, if it occurs at all, may differ from the formation of anthocyanin metabolons in lamiales species. Additionally, *FNSII* may not be required for the efficient synthesis of anthocyanins. These observations illustrate possible variations in flavonoid metabolon structures among different plant species.

EXPERIMENTAL PROCEDURES

Plant materials

The Snapshot series of snapdragon cultivars (Snapshot Red, Snapshot Red Bicolor, Snapshot Burgundy, Snapshot Orange, Snapshot Pink, Snapshot White and Snapshot Yellow) was obtained from Dainichi Shokai (Koga, Ibaraki, Japan). Meanwhile, the snapdragon cultivars Yellow Butterfly and Floral Shower Red were purchased from a local market in Sendai, Japan. Snapdragons flower development was divided into six stages as previously described (Sato *et al.*, 2001; Figure 7).

Snapdragon and torenia flavonoid enzyme cDNAs

The complete open reading frames encoding the following flavonoid enzymes (DDBJ/ENA/GenBank accession numbers in parentheses) were cloned into the pGEM-T Easy vector (Promega, Madison, WI, USA), and the nucleotide sequence of the inserted DNA was confirmed by sequencing: *AmCHS1* (X03710) (Hatayama *et al.*, 2006), *AmCHI1* (AB861648) (Fujino *et al.*, 2014), *AmFNSII* (AB028151) (Akashi *et al.*, 1999), *AmF3H* (LC194907), *AmDFR* (P14721) (Beld *et al.*, 1989), *AmC4'GT* (AB198665) (Ono *et al.*, 2006), *AmAS1* (AB044884) (Nakayama *et al.*, 2000), *AmF3'H* (DQ272592) (Schwinn *et al.*, 2006), *ThCHS1* (AB106522) (Fukusaki *et al.*, 2004), *ThCHI1_1* (LC194908), *ThCHI1_2* (LC194909), *ThFNSII* (AB028152) (Akashi *et al.*, 1999), *ThF3H* (AB211958), *ThDFR* (AB012924) (Suzuki *et al.*, 2000), *ThANS* (identical to *Torenia fournieri* ANS; AB044091) (Nakamura *et al.*, 2006), *THF3'H* (AB057672) (Ueyama *et al.*, 2002) and *ThF3'5'H* (AB012925) (Suzuki *et al.*, 2000). The *AmF3H* and *AmDFR* cDNAs were kindly provided by Dr Yuji Kishima, Hokkaido University.

Construction of plasmids for the SU system and protein–protein interaction assays

Protein–protein interactions between *AmFNSII* (or *ThFNSII*) and other flavonoid enzymes were identified in the SU system with the DUALmembrane Kit 3 (Dualsystems Biotech, Zurich, Switzerland). The full-length *AmFNSII* and *ThFNSII* genes (without a translation stop codon) were obtained by digesting the corresponding pGEM-T Easy vector constructs with the restriction enzyme *SfI*. The digested products were gel-purified and subcloned into the *SfI* sites of the pBT3-SUC vector included in the kit. This vector enabled the production of *AmFNSII* and *ThFNSII*

with the SUC2 peptide and C_{ub}-LexA-VP16 protein added to the N- and C-termini, respectively. To construct the plasmids expressing N_{ub}G-X and X-N_{ub}G, the *Sfi*I-digested and *Spel*/*Sfi*I-digested cDNA fragments encoding a flavonoid enzyme (X, see Results for details) were subcloned into the pPR3-N and pPR3-C vectors, respectively.

The *S. cerevisiae* strain NMY51 [MAT α his3Δ200 trp1-901 leu2-3,112 ade2 LYS2::(lexAop)4-HIS3 ura3::(lexAop)8-lacZ ade2::(lexAop)8-ADE2 GAL4], which was included in the DUAL membrane Kit 3, was transformed with one of the following pairs of plasmids [derivatives of pBT3-SUC and pPR3-N; derivatives of pBT3-SUC and pPR3-C; or, as a positive control, pOst1-NubI (plasmid expressing a fusion protein comprising the yeast resident ER protein Ost1 and the wild-type Nub portion of yeast ubiquitin) and derivatives of pBT3-SUC] using the polyethylene glycol–lithium acetate method described in the manufacturer's instructions. Interactions between the tested proteins were also determined based on the growth and β-galactosidase activities of the transformed cells (Waki *et al.*, 2016). Specifically, a single colony on synthetic dropout (SD) agar medium lacking tryptophan and leucine (SD/-WL) was transferred to liquid SD/-WL medium, which was then incubated at 30°C overnight with shaking. Cells were collected by centrifugation (6000 *g*, 5 min) and then suspended in sterile water to an optical turbidity at 600 nm (OD₆₀₀) of 1.0. We then placed 5-μl aliquots of fivefold serial dilutions of the cell suspension on agar-solidified SD/-WL, SD/-WLH (SD/-WL lacking histidine), SD/-WLHAdE (SD/-WLH lacking adenine) and SD/-WLHAdE+AT [SD/-WLHAdE supplemented with 1–25 mM 3AT (Sigma, St Louis, MO, USA)]. The inoculated media were incubated at 30°C for 2–4 days.

Analysis of DFR binding to FNSII in the presence of CHI

Full-length *AmCHI* cDNA was amplified by PCR to introduce *Nhe*I and *Xma*I sites to the 5'- and 3'-termini of the cDNA, respectively, using pBT3SUC-AmCHI as the template. Full-length *AmDFR* cDNA was also obtained in a similar manner using pBT3SUC-AmDFR as the template. The amplified cDNAs were digested with *Nhe*I and *Xma*I, and then cloned into the *Nhe*I/*Xma*I-digested pgK426 vector (Ishii *et al.*, 2009) to obtain pgK426-AmCHI and pgK426-AmDFR.

Saccharomyces cerevisiae NMY51 cells harboring derivatives of pBT3-SUC and pPR3-N were transformed with pgK426, pgK426-AmCHI or pgK426-AmDFR, and then grown on SD agar medium lacking tryptophan, leucine and uracil (SD/-WLU). A single colony growing on the agar medium was subsequently transferred to liquid SD/-WLU medium, which was then incubated at 30°C overnight with shaking. Cells were collected by centrifugation and suspended in sterile water to an OD₆₀₀ of 1.0. Then, 5-μl aliquots of a fivefold serial dilution of the cell suspension were placed on agar-solidified SD/-WLU, SD/-WLUHAdE, SD/-WLUHAdE+10 mM AT and SD/-WLUHAdE+25 mM AT media. Cells were grown at 30°C for 2–4 days.

Y2H assays

Yeast two-hybrid assays were completed using the Matchmaker Gold Yeast Two-Hybrid System (Clontech, Mountain View, CA, USA) and a slightly modified version of a published procedure (Waki *et al.*, 2016). Specifically, *S. cerevisiae* strain AH109 (Clontech) was transformed with each pair of plasmids encoding proteins to be tested for a possible interaction.

BiFC and subcellular localization studies

For BiFC assays, the binary vector pDOE-05 (Gookin and Assmann, 2014) was used to express the proteins of interest, which were

fused with NmVen210 and CVen210 (see also Results). For example, *AmCHS*, *AmCHI* and *AmDFR* cDNAs were digested with *Nco*I/*Spel* and ligated into multiple cloning site (MCS) 1 of pDOE-05 to generate pDOE05-CHS, pDOE05-CHI and pDOE05-DFR, respectively. *PpuMI*/*Aat*II-digested *AmFNSII* cDNA was then inserted into the *San*DI/*Aat*II sites in the MCS3 of these plasmids to produce pDOE05-CHS-FNSII, pDOE05-CHI-FNSII and pDOE05-DFR-FNSII, respectively. The binary plasmid ER-rb (Nelson *et al.*, 2007) was used to express an ER marker protein (mCherry-HDEL).

Agrobacterium tumefaciens GV3101 (pMP90) cells harboring one of the pDOE derivatives were incubated at 28°C for 1 day with 20 μM acetoxyrингone. Cells were collected by centrifugation, washed with infiltration buffer [10 mM MES-KOH (pH 5.7), 10 mM MgCl₂ and 200 μM acetoxyrингone], and resuspended in the same buffer to an OD₆₀₀ of 0.05–0.5. Wild-type *N. benthamiana* tobacco plants grown at 25°C for 4–5 weeks under long-day conditions (16-h light/8-h dark photoperiod) were agroinfiltrated with the pDOE derivatives. The plants were then incubated at 25°C under long-day conditions for 2 days.

Tobacco leaf pieces were mounted directly on glass slides or glass-bottom dishes with a drop of water and then covered with glass coverslips. Fluorescence in the cells of tobacco leaves was observed using a TCS-SP8 confocal laser-scanning microscope (Leica, Mannheim, Germany) with a white light laser and a HyD detector. The mTq2 fluorescence was detected using excitation and emission wavelengths of 458 and 460–500 nm, respectively. The mVen fluorescence was observed with excitation and emission wavelengths of 514 and 520–560 nm, respectively. The mCherry fluorescence was detected with excitation and emission wavelengths of 594 and 600–640 nm. Transmission images were recorded using a photomultiplier tube-type detector. Each image was collected in the 'between lines' sequential scanning mode.

To study the subcellular localization of AmFNSII, AmCHS1, AmCHI1, AmF3H and AmDFR, the binary vector pDOE-13 (Gookin and Assmann, 2014) was used to express their chimeras with mTq2 or mVen. The *AmCHS1*, *AmCHI1*, *AmF3H* and *AmDFR* cDNAs were digested with *Nco*I/*Spel* and ligated into MCS1 of pDOE-13 to generate pDOE13-CHS, pDOE13-CHI, pDOE13-F3H and pDOE13-DFR, respectively. *PpuMI*/*Aat*II-digested *AmFNSII* was inserted into the *San*DI/*Aat*II sites in MCS3 of pDOE-13 to obtain pDOE13-FNSII. The transformation of *A. tumefaciens* cells with one of these plasmids, the agroinfiltration of *N. benthamiana* leaves with the resulting bacterial cells, and the observation of fluorescence from transformed *N. benthamiana* cells by confocal laser microscopy were conducted as described above.

Differential centrifugation

Snapdragon petals (1 g, fresh weight; calyces removed) were ground to a powder in liquid nitrogen using a mortar and a pestle. The powder was suspended in 2 ml of 20 mM potassium phosphate, pH 8.0, containing the recommended amount of a proteinase inhibitor cocktail (Nacalai Tesque, Kyoto, Japan) and 20 mg polyvinylpolypyrrolidone. The resulting petal homogenate was centrifuged at 300 *g* for 5 min at 4°C. The supernatant was collected and centrifuged at 15 000 *g* for 15 min at 4°C. The resulting precipitate was washed with the same buffer (without polyvinylpolypyrrolidone) and used as the insoluble membrane fraction. The supernatant was then subjected to ultracentrifugation at 100 000 *g* for 60 min at 4°C, and the supernatant was collected and used as the soluble fraction. The precipitate was resuspended in 300 μl of 20 mM potassium phosphate, pH 8.0, containing the recommended amount of a proteinase inhibitor cocktail, and centrifuged again at 100 000 *g* for 60 min at 4°C. The

resulting precipitate was re-suspended in 50 µl of 20 mM potassium phosphate, pH 8.0, containing 1 mM phenylmethylsulfonyl fluoride, and then used as the petal microsome fraction.

SDS-PAGE and Western blotting

Sodium dodecyl sulfate-polyacrylamide gel electrophoresis (SDS-PAGE) was conducted as described by Laemmli (1970). Equal amounts of proteins (typically 10 µg per lane) were electrophoresed simultaneously. The proteins were visualized by silver staining and/or staining with Coomassie Brilliant Blue. For immunoblot analyses, proteins in the SDS-PAGE gel were transferred to an Immobilon-P membrane (Millipore, Billerica, MA, USA) by electroblotting using a Trans-Blot SD Semi-Dry Electrophoretic Transfer Cell (Bio-Rad, Hercules, CA, USA). The membrane was then blocked overnight at 4°C in an appropriately diluted blocking reagent (PVDF Blocking Reagent for Can Get Signal; Toyobo, Osaka, Japan). The membrane was washed with PBS-T (4.3 mM Na₂HPO₄, 1.4 mM KH₂PO₄, 2.7 mM KCl, 137 mM NaCl and 0.1% Tween 20) for 25 min, and then probed with appropriate dilutions of a primary antibody [immunoglobulin G (IgG), rabbit] and the peroxidase-conjugated secondary goat anti-rabbit IgG (Medical & Biological Laboratories, Nagoya, Japan). The immune complexes were visualized using the ECL Prime Western Blotting Detection Reagent (GE Healthcare Life Sciences, Piscataway, NJ, USA) following the manufacturer's instructions. The immunoblots were quantified using Image J software, and an abundance ratio (soluble: microsomal, mol/mol) was estimated for each enzyme based on protein concentrations and the volumes of the soluble and microsomal fractions, assuming the microsomal fraction yield was 100%.

Preparation of antibodies

To obtain anti-AmCHS1 and anti-AmCHI1 antibodies, electrophoretically homogeneous preparations of the non-denatured forms of recombinant AmCHS1 (Hatayama *et al.*, 2006) and AmCHI1 (Fujino *et al.*, 2014) were used to immunize female Japanese white rabbits by an intradermal injection at multiple sites according to standard protocols (Vaitukaitis, 1981). To obtain anti-AmFNSII and anti-DFR antibodies, the peptides corresponding to amino acid residues 469–487 of AmFNS and residues 334–352 of AmDFR, which were predicted to serve as epitopes, were used to immunize female Japanese white rabbits.

The initial injection was administered in complete Freund's Adjuvant with all subsequent immunizations in incomplete Freund's Adjuvant. The collected serum was subjected to ammonium sulfate fractionation, and the precipitate from the 0–50% saturation fraction was dissolved in 5 ml of 20 mM sodium phosphate buffer, pH 7.0. The protein solution was applied to a Protein A-Sepharose column (3 ml; GE HealthCare Life Sciences) that had been equilibrated with the same buffer. After washing the column with the same buffer, IgG was eluted with 0.1 M sodium citrate buffer, pH 4.0. The eluate containing IgG was immediately dialyzed against 20 mM sodium phosphate buffer, pH 7.0. For anti-AmFNS and anti-DFR antibodies, the resulting IgG was purified by affinity chromatography using an agarose column to which the epitope peptides were immobilized.

Flavonoid analysis

Petals (with calyces removed) were frozen in liquid nitrogen and then lyophilized. The freeze-dried petals (0.1 g) were then pulverized with 1 ml extraction solvent (0.1% trifluoroacetic acid:

acetonitrile = 1:1) using the MBS200 Multi-Beads Shocker (Yasui Kikai, Osaka, Japan) at 2000 rpm for 30 sec. The homogenate was centrifuged at 10 000 *g* for 2 min. The supernatant was passed through a 0.22-µm Chromafil O-20/15MS filter (Macherey-Nagel GmbH, Düren, Germany) and used as the petal extract for the flavonoid analysis by HPLC. To analyze flavones and flavonols, the petal extracts were mixed with an equal volume of 2 M HCl and then incubated at 100°C for 1 h (Hertog *et al.*, 1992). The resulting aglycons were analyzed by HPLC. Anthocyanins and aurones in the petal extracts were determined as their 3-rutinosides and 6-glucosides, respectively. The anthocyanin and aurone contents were confirmed after an acid hydrolysis of their glycosides with 1 M HCl at 100°C for 1 h.

The HPLC analyses were conducted using a Shimadzu LC Solution system (Shimadzu, Kyoto, Japan) as follows: column, YMC J'sphere ODS M80 (4.6 × 150 mm; YMC, Kyoto, Japan); flow rate, 0.5 ml min⁻¹; solvent A, 0.1% (by vol.) trifluoroacetic acid in H₂O; solvent B, 0.1% trifluoroacetic acid in a 9:1 (by vol.) mixture of acetonitrile and H₂O. After the sample was injected onto the column equilibrated with 15% B (by vol.), the column was initially developed isocratically with 15% B for 5 min, followed by a linear gradient from 15% B to 55% B over 35 min, followed by a linear gradient from 55% B to 100% B over 1 min. The column was then washed isocratically with 100% B for 5 min, followed by a linear gradient from 100% B to 15% B over 1 min. There was a 13-min delay before the next injection to ensure the column was re-equilibrated. Chromatograms were obtained using the SPD-M20A photodiode array spectrophotometer (200–650 nm; Shimadzu). The retention times and detection wavelengths for aurones, flavones and anthocyanins under these HPLC conditions are summarized in Table S3. Pigment abundances were determined based on peak integrals using authentic standards as calibrators.

qRT-PCR

Snapdragon petals (with calyces removed) at different stages of flower development were frozen in liquid nitrogen, and pulverized with a mortar and pestle. Total RNA was extracted from the pulverized petals using the Extract-A-Plant RNA Isolation Kit (Clontech). Contaminating DNA was eliminated by treating the extracted RNA with RNase-free DNase I (Roche Diagnostics GmbH, Mannheim, Germany) in the presence of a recombinant ribonuclease inhibitor (Takara Bio, Shiga, Japan) at 37°C for 30 min. The purified RNA was used as the template for a reverse transcription, which was completed with the PrimeScript RT reagent kit (Perfect Real Time; Takara Bio) according to the manufacturer's guidelines. The qRT-PCR analyses of *AmFNSII*, *AmCHS1*, *AmC4'GT*, *AmCHI1*, *AmF3H*, *AmDFR*, *AmF3'H* and *AmUBQ* (ubiquitin) expression levels were completed with the SYBR Select Master Mix (Life Technologies) and an Eco Real-time PCR system (Illumina, San Diego, CA, USA). Details regarding the gene-specific primers and PCR conditions are provided in Table S4.

ACKNOWLEDGEMENTS

The authors are grateful to Dr Kazuo Ichimura, NARO Institute of Floricultural Science, and Dr Yuji Kishima, Hokkaido University, for their support and fruitful discussions. The authors are indebted to Dr Akira Kanazawa, Hokkaido University, and Dr Takeshi Yoshizumi, RIKEN, for their guidance concerning virus-induced gene silencing and RNAi via peptide-based gene delivery, respectively. The authors gratefully acknowledge two anonymous reviewers for helpful comments regarding the manuscript. This study was supported by JSPS KAKENHI Grant Number JP21310135, and grants

from the 160th Committee on Plant Biotechnology for the Environment, Food and Resources, Japan Society for the Promotion of Science as well as the Japan Foundation for Applied Enzymology. The authors thank Edanz Group (www.edanzediting.com/ac) for editing this manuscript.

CONFLICT OF INTEREST

The authors declare no conflicts of interest.

SUPPORTING INFORMATION

Additional Supporting Information may be found in the online version of this article.

Figure S1. Interactions among snapdragon flavonoid enzymes as determined by the SU system.

Figure S2. Results of Y2H assays used to screen for interactions of (a) CHS, (b) CHI, (c) F3H, (d) DFR with other cytoplasmic flavonoid enzymes in snapdragon.

Figure S3. Example of the negative controls in the BiFC assays used to detect binary interactions among snapdragon flavonoid enzymes in *benthamiana* tobacco leaf cells.

Figure S4. Control experiments confirming the lack of contaminating cytoplasmic proteins in the microsomal fraction.

Figure S5. Selected snapdragon cultivars used in this study (Snapshot series).

Figure S6. Results of Y2H assays used to screen for interactions of (a) CHS, (b) CHI1_1, (c) CHI1_2, (d) F3H, (e) DFR and (f) ANS with cytoplasmic flavonoid enzymes in *torenia*.

Figure S7. Correlation between anthocyanin and flavone content in the petals of Cy-accumulating snapdragon cultivars (red circles: Snapshot Red, Snapshot Red Bicolor and FloralShower Red) and Pg-accumulating cultivars (pink circles: Snapshot Burgundy, Snapshot Orange and Snapshot Pink).

Table S1. Results of binary protein–protein interaction assays using the SU and Y2H systems involving (a) snapdragon and (b) *torenia* flavonoid enzymes

Table S2. Flavonoid contents of some commercial snapdragon varieties

Table S3. Identification of flavonoids by HPLC

Table S4. Nucleotide sequences of qRT-PCR primers

REFERENCES

- Akashi, T., Fukuchi-Mizutani, M., Aoki, T., Ueyama, Y., Yonekura-Sakakibara, K., Tanaka, Y., Kusumi, T. and Ayabe, S. (1999) Molecular cloning and biochemical characterization of a novel cytochrome P450, flavone synthase II, that catalyzes direct conversion of flavanones to flavones. *Plant Cell Physiol.*, **40**, 1182–1186. <https://doi.org/10.1093/oxfordjournals.pcp.a029505>
- Andersen, Ø.M. and Markham, K.R. (2006) Preface. In *Flavonoids: Chemistry, Biochemistry and Applications*. (Andersen, Ø. M. and Markham, K. R., eds). Boca Raton, FL: CRC Press.
- Asen, S., Norris, K.H. and Stewart, R.N. (1972) Copigmentation of aurone and flavone from petals of *Antirrhinum majus*. *Phytochemistry*, **11**, 2739–2741. [https://doi.org/10.1016/S0031-9422\(00\)86505-X](https://doi.org/10.1016/S0031-9422(00)86505-X)
- Bassard, J.-E., Richert, L., Geerinck, J. et al. (2012) Protein–protein and protein–membrane associations in the lignin pathway. *Plant Cell*, **24**, 4465–4482. <https://doi.org/10.1105/tpc.112.102566>
- Bassard, J.E., Möller, B.L. and Laursen, T. (2017) Assembly of dynamic P450-mediated metabolons – order versus chaos. *Curr. Mol. Biol. Rep.*, **3**, 37–51. <https://doi.org/10.1007/s40610-017-0053-y>
- Beld, M., Martin, C., Huits, H., Stuitje, A.R. and Gerats, A.G. (1989) Flavonoid synthesis in *Petunia hybrida*: partial characterization of dihydroflavonol-4-reductase genes. *Plant Mol. Biol.*, **13**, 491–502. <https://doi.org/10.1007/BF00027309>
- Chien, C.T., Bartel, P.L., Sternglanz, R. and Fields, S. (1991) The two-hybrid system: a method to identify and clone genes for proteins that interact with a protein of interest. *Proc. Natl Acad. Sci. USA*, **88**, 9578–9582. <https://doi.org/10.1073/pnas.88.21.9578>
- Crosby, K.C., Pietraszewska-Bogiel, A., Gadella, T.W. Jr and Winkel, B.S. (2011) Förster resonance energy transfer demonstrates a flavonoid metabolon in living plant cells that displays competitive interactions between enzymes. *FEBS Lett.*, **585**, 2193–2198. <https://doi.org/10.1016/j.febslet.2011.05.066>
- Dastmalchi, M., Bernards, M.A. and Dhaubhadel, S. (2016) Twin anchors of the soybean isoflavonoid metabolon: evidence for tethering of the complex to the endoplasmic reticulum by IFS and C4H. *Plant J.*, **85**, 689–706. <https://doi.org/10.1111/tpj.13137>
- Deguchi, A., Ohno, S., Hosokawa, M., Tatsuzawa, F. and Doi, M. (2013) Endogenous post-transcriptional gene silencing of flavone synthase resulting in high accumulation of anthocyanins in black dahlia cultivars. *Planta*, **237**, 1325–1335. <https://doi.org/10.1007/s00425-013-1848-6>
- Forkmann, G. and Stotz, G. (1981) Genetic control of flavanone 3-hydroxylase activity and flavonoid 3'-hydroxylase activity in *Antirrhinum majus* (Snapdragon). *Z. Naturforsch.*, **36C**, 411–416.
- Fujino, N., Yamazaki, T., Li, Y., Kera, K., Furuhashi, E., Yamashita, T., Morita, Y., Nakayama, M., Takahashi, S. and Nakayama, T. (2014) cDNA cloning and characterization of chalcone isomerase-fold proteins from snapdragon (*Antirrhinum majus* L.) flowers. *Plant Biotechnol.*, **31**, 105–114. <https://doi.org/10.5511/plantbiotechnology.14.0109c>
- Fukasaki, E.-i., Kawasaki, K., Kajiyama, S., An, C.-I., Suzuki, K., Tanaka, Y. and Kobayashi, A. (2004) Flower color modulations of *Torenia hybrida* by downregulation of chalcone synthase genes with RNA interference. *J. Biotech.*, **111**, 229–240. <https://doi.org/10.1016/j.jbiotec.2004.02.019>
- Fulton, A.B. (1982) How crowded is the cytoplasm? *Cell*, **30**, 345–347. [https://doi.org/10.1016/0092-8674\(82\)90231-8](https://doi.org/10.1016/0092-8674(82)90231-8)
- Ghosh, I., Hamilton, A.D. and Regan, L. (2000) Detecting protein–protein interactions with a green fluorescent protein fragment reassembly trap: scope and mechanism. *J. Am. Chem. Soc.*, **127**, 146–157.
- Gookin, T.E. and Assmann, S.M. (2014) Significant reduction of BiFC non-specific assembly facilitates in planta assessment of heterotrimeric G-protein interactors. *Plant J.*, **80**, 553–567. <https://doi.org/10.1111/tpj.12639>
- Graham, J.W., Williams, T.C., Morgan, M., Fernie, A.R., Ratcliffe, R.G. and Sweetlove, L.J. (2007) Glycolytic enzymes associate dynamically with mitochondria in response to respiratory demand and support substrate channeling. *Plant Cell*, **19**, 3723–3738. <https://doi.org/10.1105/tpc.107.053371>
- Hatayama, M., Ono, E., Yonekura-Sakakibara, K., Tanaka, Y., Nishino, T. and Nakayama, T. (2006) Biochemical characterization and mutational studies of a chalcone synthase from yellow snapdragon (*Antirrhinum majus*) flowers. *Plant Biotech.*, **23**, 373–378. <https://doi.org/10.5511/plantbiotechnology.23.373>
- Hertog, M.G.L., Hollman, P.C.H. and Venema, D.P. (1992) Optimization of a Quantitative HPLC determination of potentially anticarcinogenic flavonoids in vegetables and fruits. *J. Agr. Food Chem.*, **40**, 1591–1598. <https://doi.org/10.1021/jf00021a023>
- Hrazdina, G. and Wagner, G.J. (1985) Metabolic pathways as enzyme complexes: evidence for the synthesis of phenylpropanoids and flavonoids on membrane associated enzyme complexes. *Arch. Biochem. Biophys.*, **237**, 88–100. [https://doi.org/10.1016/0003-9861\(85\)90257-7](https://doi.org/10.1016/0003-9861(85)90257-7)
- Hrazdina, G., Zobel, A.M. and Hoch, H.C. (1987) Biochemical, immunological, and immunocytochemical evidence for the association of chalcone synthase with endoplasmic reticulum membranes. *Proc. Natl Acad. Sci. USA*, **84**, 8966–8970. <https://doi.org/10.1073/pnas.84.24.8966>
- Hudson, A., Critchley, J. and Erasmus, Y. (2008) The genus *Antirrhinum* (snapdragon): a flowering plant model for evolution and development. *Cold Spring Harb. Protoc.*, doi:10.1101/pdb.em0100.
- Ishii, J., Izawa, K., Matsumura, S., Wakamura, K., Tanino, T., Tanaka, T., Ogino, C., Fukuda, H. and Kondo, A. (2009) A simple and immediate method for simultaneously evaluating expression level and plasmid maintenance in yeast. *J. Biochem.*, **145**, 701–708. <https://doi.org/10.1093/jb/mvp028>
- Iyer, K., Burkle, L., Auerbach, D., Thaminy, S., Dinkel, M., Engels, K. and Stagljar, I. (2005) Utilizing the split-ubiquitin membrane yeast two-hybrid system to identify protein–protein interactions of integral membrane proteins. *Sci. STKE*, **2005**, pl3.

- Jackson, D., Roberts, K. and Martin, C. (1992) Temporal and spatial control of expression of anthocyanin biosynthetic genes in developing flowers of *Antirrhinum majus*. *Plant J.*, **2**, 425–434. <https://doi.org/10.1111/j.1365-313X.1992.00425.x>
- Jez, J.M., Bowman, M.E., Dixon, R.A. and Noel, J.P. (2000) Structure and mechanism of the evolutionarily unique plant enzyme chalcone isomerase. *Nature Struct. Biol.*, **7**, 786–791.
- Jorgensen, K., Rasmussen, A.V., Morant, M., Nielsen, A.H., Bjarnholt, N., Zagrobelny, M., Bak, S. and Møller, B.L. (2005) Metabolon formation and metabolic channeling in the biosynthesis of plant natural products. *Curr. Opin. Plant Biol.*, **8**, 280–291. <https://doi.org/10.1016/j.pbi.2005.03.014>
- Laemmli, U.K. (1970) Cleavage of structural proteins during the assembly of the head of bacteriophage T4. *Nature*, **227**, 680–685. <https://doi.org/10.1038/227680a0>
- Laursen, T., Møller, B.L. and Bassard, J.E. (2015) Plasticity of specialized metabolism as mediated by dynamic metabolons. *Trends Plant Sci.*, **20**, 20–32. <https://doi.org/10.1016/j.tplants.2014.11.002>
- Laursen, T., Borch, J., Knudsen, C. et al. (2016) Characterization of a dynamic metabolon producing the defense compound dhurrin in sorghum. *Science*, **354**, 890–893. <https://doi.org/10.1126/science.aag2347>
- Martin, C., Prescott, A., Mackay, S., Bartlett, J. and Vrijlandt, E. (1991) Control of anthocyanin biosynthesis in flowers of *Antirrhinum majus*. *Plant J.*, **1**, 37–49. <https://doi.org/10.1111/j.1365-313X.1991.00037.x>
- Møller, B.L. (2010) Plant science. Dynamic metabolons. *Science*, **330**, 1328–1329.
- Mouradov, A. and Spangenberg, G. (2014) Flavonoids: a metabolic network mediating plants adaptation to their real estate. *Frontiers Plant Sci.*, **5**, 620. doi: 10.3389/fpls.2014.00620.
- Nakamura, N., Fukuchi-Mizutani, M., Miyazaki, K., Suzuki, K. and Tanaka, Y. (2006) RNAi suppression of the anthocyanidin synthase gene in *Torenia hybrida* yields white flowers with higher frequency and better stability than antisense and sense suppression. *Plant Biotechnol.*, **23**, 13–17. <https://doi.org/10.5511/plantbiotechnology.23.13>
- Nakayama, T., Yonekura-Sakakibara, K., Sato, T. et al. (2000) Aureusidin synthase: a polyphenol oxidase homolog responsible for flower coloration. *Science*, **290**, 1163–1166. <https://doi.org/10.1126/science.290.5549.1163>
- Nakayama, T., Sato, T., Fukui, Y., Yonekura-Sakakibara, K., Hayashi, H., Tanaka, Y., Kusumi, T. and Nishino, T. (2001) Specificity analysis and mechanism of aurone synthesis catalyzed by aureusidin synthase, a polyphenol oxidase homolog responsible for flower coloration. *FEBS Lett.*, **499**, 107–111. [https://doi.org/10.1016/S0014-5793\(01\)02529-7](https://doi.org/10.1016/S0014-5793(01)02529-7)
- Nelson, B.K., Cai, X. and Nebenführ, A. (2007) A multicolored set of *in vivo* organelle markers for co-localization studies in *Arabidopsis* and other plants. *Plant J.*, **51**, 1126–1136. <https://doi.org/10.1111/j.1365-313X.2007.03212.x>
- Noguchi, A., Horikawa, M., Fukui, Y., Fukuchi-Mizutani, M., Iuchi-Okada, A., Ishiguro, M., Kiso, Y., Nakayama, T. and Ono, E. (2009) Local differentiation of sugar donor specificity of flavonoid glycosyltransferase in Lamiaceae. *Plant Cell*, **21**, 1556–1572. <https://doi.org/10.1105/tpc.108.063826>
- Ono, E., Fukuchi-Mizutani, M., Nakamura, N., Fukui, Y., Yonekura-Sakakibara, K., Yamaguchi, M., Nakayama, T., Tanaka, T., Kusumi, T. and Tanaka, Y. (2006) Yellow flowers generated by expression of the aurone biosynthetic pathway. *Proc. Natl Acad. Sci. USA*, **103**, 11 075–11 080. <https://doi.org/10.1073/pnas.0604246103>
- Ovadi, J. (1991) Physiological significance of metabolic channelling. *J. Theor. Biol.*, **152**, 1–22. [https://doi.org/10.1016/S0022-5193\(05\)80500-4](https://doi.org/10.1016/S0022-5193(05)80500-4)
- Ovadi, J. and Saks, V. (2004) On the origin of intracellular compartmentation and organized metabolic systems. *Mol. Cell. Biochem.*, **256–257**, 5–12. <https://doi.org/10.1023/B:MCB.0000009855.14648.2c>
- Ovadi, J. and Srere, P.A. (2000) Macromolecular compartmentation and channelling. *Int. Rev. Cytol.*, **192**, 255–280.
- Petit, P., Granier, T., d'Estaintot, B.L., Manigand, C., Bathany, K., Schmitter, J.-M., Lauvergeat, V., Hamdi, S. and Gallois, B. (2007) Crystal structure of grape dihydroflavonol 4-reductase, a key enzyme in flavonoid biosynthesis. *J. Mol. Biol.*, **368**, 345–357.
- Ralston, L. and Yu, O. (2006) Metabolons involving plant cytochrome P450s. *Phytochem. Rev.*, **5**, 459–472. <https://doi.org/10.1007/s11101-006-9014-4>
- Sasaki, N. and Nakayama, T. (2015) Achievements and perspectives in biochemistry concerning anthocyanin modification for blue flower coloration. *Plant Cell Physiol.*, **56**, 28–40. <https://doi.org/10.1093/pcp/pcu097>
- Sato, T., Nakayama, T., Kikuchi, S., Fukui, Y., Yonekura-Sakakibara, K., Ueda, T., Nishino, T., Tanaka, Y. and Kusumi, T. (2001) Enzymatic formation of aurones in the extracts of yellow snapdragon flowers. *Plant Sci.*, **160**, 229–236. [https://doi.org/10.1016/S0168-9452\(00\)00385-X](https://doi.org/10.1016/S0168-9452(00)00385-X)
- Schwarz-Sommer, Z., Davies, B. and Hudson, A. (2003) An everlasting pioneer: the story of *Antirrhinum* research. *Nat. Rev. Genet.*, **4**, 657–666.
- Schwinn, K., Venail, J., Shang, Y.J., Mackay, S., Alm, V., Butelli, E., Oyama, R., Bailey, P., Davies, K. and Martin, C. (2006) A small family of MYB-regulatory genes controls floral pigmentation intensity and patterning in the genus *Antirrhinum*. *Plant Cell*, **18**, 831–851. <https://doi.org/10.1105/tpc.105.039255>
- Srere, P.A. (2000) Macromolecular interactions: tracing the roots. *Trends Biochem. Sci.*, **25**, 150–153. [https://doi.org/10.1016/S0968-0004\(00\)01550-4](https://doi.org/10.1016/S0968-0004(00)01550-4)
- Stafford, H.A. (1974) The metabolism of aromatic compounds. *Ann. Rev. Plant Physiol.*, **25**, 459–486. <https://doi.org/10.1146/annurev.pp.25.060174.002331>
- Stickland, R.G. and Harrison, B.J. (1974) Precursors and genetic control of pigmentation. I. Induced biosynthesis of pelargonidin, cyanidin and delphinidin in *Antirrhinum majus*. *Heredity*, **33**, 108–112. <https://doi.org/10.1038/hdy.1974.73>
- Suzuki, K., Xue, H.M., Tanaka, Y., Fukui, Y., Fukuchi-Mizutani, M., Murakami, Y., Katsumoto, Y., Tsuda, S. and Kusumi, T. (2000) Flower color modifications of *Torenia hybrida* by cosuppression of anthocyanin biosynthesis genes. *Mol. Breeding*, **6**, 239–246. <https://doi.org/10.1023/A:1009678514695>
- Sweetlove, L.J. and Fernie, A.R. (2013) The spatial organization of metabolism within the plant cell. *Annu. Rev. Plant Biol.*, **64**, 723–746. <https://doi.org/10.1146/annurev-arplant-050312-120233>
- Tanaka, Y. and Brugliera, F. (2013) Flower colour and cytochromes P450. *Philos. Trans. R. Soc. B*, **368**, 20120 432. <https://doi.org/10.1098/rstb.2012.0432>
- Thill, J., Miosic, S., Ahmed, R., Schlangen, K., Muster, G., Stich, K. and Halbwirth, H. (2012) 'Le Rouge et le Noir': a decline in flavone formation correlates with the rare color of black dahlia (*Dahlia variabilis* hort.) flowers. *BMC Plant Biol.*, **12**, 225. <https://doi.org/10.1186/1471-2229-12-225>
- Toki, K. (1988) Studies on the flower pigments in snapdragon, *Antirrhinum majus* L. *Bull. Facult. Hort. MinamiKyushu Univ.*, **18**, 1–68 (in Japanese).
- Ueyama, Y., Suzuki, K., Fukuchi-Mizutani, M., Fukui, Y., Miyazaki, K., Ohkawa, H., Kusumi, T. and Tanaka, Y. (2002) Molecular and biochemical characterization of torenia flavonoid 3'-hydroxylase and flavone synthase II and modification of flower color by modulating the expression of these genes. *Plant Sci.*, **163**, 253–263. [https://doi.org/10.1016/S0168-9452\(02\)00098-5](https://doi.org/10.1016/S0168-9452(02)00098-5)
- Vaitukaitis, J.L. (1981) Production of antisera with small doses of immunogen: multiple intradermal injections. *Methods Enzymol.*, **73**, 46–52. [https://doi.org/10.1016/0076-6879\(81\)73055-6](https://doi.org/10.1016/0076-6879(81)73055-6)
- Verkman, A.S. (2002) Solute and macromolecule diffusion in cellular aqueous compartments. *Trends Biochem. Sci.*, **27**, 27–33. [https://doi.org/10.1016/S0968-0004\(01\)02003-5](https://doi.org/10.1016/S0968-0004(01)02003-5)
- Waki, T., Yoo, D., Fujino, N. et al. (2016) Identification of protein-protein interactions of isoflavonoid biosynthetic enzymes with 2-hydroxyisoflavanone synthase in soybean (*Glycine max* (L.) Merr.). *Biochem. Biophys. Res. Commun.*, **469**, 546–551. <https://doi.org/10.1016/j.bbrc.2015.12.038>
- Weng, J.K. (2014) The evolutionary paths towards complexity: a metabolic perspective. *New Phytol.*, **201**, 1141–1149. <https://doi.org/10.1111/nph.12416>
- Winkel, B.S. (2004) Metabolic channelling in plants. *Annu. Rev. Plant Biol.*, **55**, 85–107. <https://doi.org/10.1146/annurev.aplant.55.031903.141714>
- Winkel-Shirley, B. (1999) Evidence for enzyme complexes in the phenylpropanoid and flavonoid pathways. *Physiol. Plant.*, **107**, 142–149. <https://doi.org/10.1034/j.1399-3054.1999.100119.x>
- Winkel-Shirley, B. (2001) Flavonoid biosynthesis. A colorful model for genetics, biochemistry, cell biology, and biotechnology. *Plant Physiol.*, **126**, 485–493. <https://doi.org/10.1104/pp.126.2.485>